

NATURAL RADIOACTIVITY LEVELS AND RADIOLOGICAL
HAZARD INDICES OF SOIL AND WATER COLLECTED FROM
KASEREM LIMESTONE QUARRY, KAPCHORWA DISTRICT,
UGANDA

BY

CHUKONDO GEOFREY


A DISSERTATION SUBMITTED TO THE GRADUATE SCHOOL IN
PARTIAL FULFILLMENT OF THE REQUIREMENTS FOR THE AWARD
OF THE DEGREE OF MASTER OF SCIENCE IN PHYSICS OF

KYAMBOGO UNIVERSITY

OCTOBER, 2017

DECLARATION

I, Chukondo Geoffrey, declare that the work presented in this dissertation is my original work and has not been presented to any academic institution for an academic award.

Signed..... 

Date..... 13/10/2017

APPROVAL

The study was conducted under our guidance and supervision. The report is hereby approved for submission to the Board of Graduate School and senate of Kyambogo University.

Signed:..........

Supervisor one: Mr. Oriada Richard Geoffrey

Physics Department,

Kyambogo University

Date:.....*October 17th 2017*.....

Signed:..........

Supervisor two: Mr. Enjiku Ben D.D

Physics Department

Kyambogo University

Date:.....*17th October 2017*.....

DEDICATION

This work is dedicated to my wife, Kissa Scovia.

ACKNOWLEDGEMENT

I wish to express my sincere gratitude to my supervisors: Oriada Richard Geoffrey and Enjiku Ben D.D for the wonderful suggestions, advice and guidance they extended to me throughout the course of the research. Their vast knowledge and experience in radiation detection, measurement and in scientific data analysis greatly enhanced my understanding of the research topic.

In a special way, I appreciate the financial support from the African Development Bank (AfDB) (HEIST project) throughout the time of study. Without their support it would have been difficult for me to finish the program

Thirdly, my heartfelt appreciation is extended to Prof. Kinyera Sam Obwoya, Prof. E.L.J.K Banda, Assoc. Prof. Dr Edward Jurua, and Prof. Eric Mucunguzi, and Kabagambe Musa for their great contributions towards this work. My thanks also go to the Physics Departments of both Kyambogo University and Makerere University especially the radiation laboratory of Makerere University where analysis of the samples took place.

The loving support of my wife, Kissa Scovia, children Chebet Joy, Chukondo Joshua and Chebet Jolly and their encouragement, patience provided motivation and determination to complete the research. Above all, I am also very grateful to my parents Kiplangat K. Nelson and Cheptai Janet for the sacrifice they made in educating me.

My thanks also go to; Ms Akoba Rashida, Habumugisha Isaac and Byamukama Abdul, members of physics department at Islamic University in Uganda who trusted me to teach their students during the course of my study. To Mr. Chelangat Kadafi, Candia John and Batya Martin I extend my gratitude for their great advice and wonderful contributions towards this work and not forgetting Doe Mudahir with whom I picked samples with for analysis. May God bless them. I sincerely appreciate the support rendered to me by my fellow course mates; Kayanja Jimmy, Musiramu Twahir, Eling Jimmy, Abson, Obillim Terece, Coope Kizito, Kamwasir Hellena and Tusimire Anita, without them writing this dissertation would have been difficult.

Above all, I thank the Almighty God, for leading me this far. I confess that without Him I would not have reached this far.

TABLE OF CONTENTS	PAGE
Declaration	i
Approval.....	ii
Dedication	iii
Acknowledgements	iv
List of figures	vii
List of tables.....	viii
Abstract	ix
CHAPTER ONE: INTRODUCTION	
1.1. Background of the Study.....	1
1.2. Statement of the Problem	5
1.3. Purpose of the Study	6
1.4. Objectives of the Study	6
1.5. Significance of the Study	6
1.6. Scope of the Study	7
CHAPTER TWO: REVIEW OF RELATED LITERATURE	
2.1. Introduction	9
2.2. Types and Sources of Radiation.....	9
2.3. Gamma-ray interaction with matter	10
2.4. Gamma-ray Spectroscopy	13
2.5. Activity concentration of gamma ray emitting radionuclides.....	17
2.6. Biological Effects of Radiation.....	22
2.7. Evaluation of Absorbed dose and Annual Effective dose.....	23
2.8. Evaluation of radiation hazard indices.....	24
2.9. Related studies on natural radioactivity	25
CHAPTER THREE: RESEARCH METHODOLOGY	
3.1. Introduction	29
3.2. Design of the study	29
3.3. Sampling and sampling techniques.....	30
3.5. Sample preparation.....	31
3.6. Measurement of Activity concentration of the Radionuclide	31



3.7	Energy calibration, resolution and efficiency of the detector	33
CHAPTER FOUR: RESULTS OF THE STUDY		
4.1	Introduction	36
4.2	Acquisition of Primary Data	36
4.2	Specific Activities of Radionuclides.....	40
4.2.1	Soil samples.....	40
4.2.2:	Water samples	42
4.3.	Dose rate values	44
4.4	Radiation hazard indices	45
CHAPTER FIVE: DISCUSSIONS, CONCLUSIONS AND RECOMMENDATIONS		
5.1.	Discussion of results	50
5.2.	Conclusion	54
5.3.	Recommendations	55
REFERENCES.....		56
APPENDIX A		62
APPENDIX B		71

LIST OF FIGURES

Figure 1.1: A pie chart showing average world percentage of radiation exposure by different sources of radiation (WHO, 2013).....	3
Figure 1.2: Google satellite map showing the location of Kaserem Limestone Quarry (source, Google maps accessed on 1 st Oct, 2017).....	7
Figure 1.3: Map of Kapchorwa District showing location of the quarry. (www.ucc.co.ug, accessed on 16 th October, 2015)	8
Figure 2.1: A graph depicting the various regions where the different gamma-ray interactions are dominant. (Attix, 1986)	11
Figure 2.2: Schematic diagram of Compton scattering, Alpen (1998)	12
Figure 2.3: Structure of Scintillator detector, Mattetnik(1995)	14
Figure 2.4: Spectrometer system for nuclear radiation (www.gammadata.net).....	15
Figure 2.5: Block diagram of a single channel analyzer, Cember (2009).....	16
Figure 2.6: Block diagram showing a multichannel analyzer MCA, Cember (2009)	16
Figure 3.0: A Schematic illustration of how the samples were collected	30
Figure 4.0: Sample spectrum for the soil sample from the central part of the quarry.....	37
Figure 4.1: A bar graph showing mean activities for the soil sampled from all locations around the quarry	41
Figure 4.2: A bar graph showing mean specific activities of radionuclides for the water samples collected	43
Figure 4.3: A graph showing absorbed dose rates in both soil and water.....	44
Figure 4.4: A graph showing Radium equivalent for both soil and water samples	46
Figure 4.5: A graph showing Hazard indices in soil and water samples	47

LIST OF TABLES

Table 3.1: Correction coefficients of radionuclides	35
Table 4.0: Radionuclides corresponding to each peak for the soil sample from location A	38
Table 4.1: Specific activities of soil samples from the central part of the quarry	39
Table 4.2: Mean activities for radionuclides in soil samples from each location around the quarry	40
Table 4.3: Overall mean and standard deviation of activities for all soil samples from the selected locations around the quarry	41
Table 4.4: Overall mean specific activities of radionuclide of water samples.	42
Table 4.5: Overall average specific activity concentration with their standard error of both soil and water from Kaserem limestone quarry area.....	43
Table 4.6: Absorbed dose rates (D) for both soil and water samples.....	44
Table 4.6: Annual effective dose rates, (AED) for both soil and water samples.	45
Table 4.7: Radium equivalent values for both soil and water samples.	45
Table 4.8: Internal hazard indices, (H_{in}) for both soil and water samples.....	46
Table 4.9: External hazard indices, (H_{ex}) for both soil and water samples.	47
Table 4.10: Comparison of activity concentrations with similar studies	48

ABSTRACT

This study was to determine the gamma ray concentration/activity due to naturally occurring radionuclides present in soil and water from Kaserem limestone quarry area in Kapchorwa District and the associated hazard indices. Reports from other studies associate limestone deposits with high concentration of radionuclides and therefore data regarding these radionuclides is useful in protecting the public from radiation exposure and minimizing risks. In this study, fifty (50) soil samples and ten (10) water samples collected from the quarry area were analyzed, with the aid of gamma spectroscopy method, using Sodium Iodide Thallium, NaI (TI) detector. The radiation parameters included radiation equivalent activity, gamma absorbed dose rate, annual effective dose and external and internal hazard indices in soil and water samples from Kaserem limestone quarry. To ensure quality control, the soil samples collected from the sites were transferred to polythene bags, labeled and double-bagged. They were then transported in boxes whose background radiation emissions were measured with an identifier while water samples were put in plastic water bottles and sealed before transportation to the laboratory. Naturally occurring radionuclides (NORM) present in soil and water samples were identified. The specific activity concentrations of ^{226}Ra , ^{232}Th , ^{238}U and ^{40}K in soil samples are: 75.71 Bq kg⁻¹, 77.01 Bq kg⁻¹, 41.07 Bq kg⁻¹ and 536.9 Bq kg⁻¹, respectively. These natural activity values were higher than the maximum permissible world average values; hence this area should be considered high background radiation area (HBRA) and the activity concentration of ^{226}Ra , ^{232}Th , ^{238}U and ^{40}K in water samples was 104.18 Bq kg⁻¹, 16.58 Bq kg⁻¹, 19.27 Bq kg⁻¹ and 22.73 Bq kg⁻¹, respectively. The average absorbed dose rates were found to be 106.39 nGy h⁻¹ for soil samples, which is about 2 times the world average of 60 nGy h⁻¹; While for water samples it was 56.44 nGy h⁻¹ which is similar to the world average absorbed dose rate of 55 nGy h⁻¹.

Assuming 33% occupancy factor, the annual average effective dose rates (AED) were calculated for human exposure to gamma radiations from the radionuclides in soil and it was found to be 0.31 mSv y⁻¹ which is below International Commission on Radiation Protection (ICRP) limit of 1 mSv y⁻¹ for exposure to members of the general public, while the value for water samples was 0.18 mSv y⁻¹ which was above the reference value of 0.12 mSv y⁻¹. While the mean radium equivalent values for soil and water samples were: 227.17 Bq kg⁻¹ and

129.64 Bq kg⁻¹ respectively which were below the reference value of 370 Bq kg⁻¹. The external and internal hazard index values were calculated and their values were 0.61 mSv y⁻¹ and 0.81 mSv y⁻¹ respectively for soil samples while 0.35 mSv y⁻¹ and 0.63 mSv y⁻¹ respectively for water samples. Since the external and internal hazard indices measured for all the samples studied were less than unity, the internationally accepted upper limit for building materials, then the soil and water from this quarry will not pose a significant radiological hazard to both the miners and the public population.

CHAPTER ONE: INTRODUCTION

1.1. Background of the Study

According to the Mining Journal, Special Publication Uganda, (2012); Uganda is endowed with a variety of minerals owing to its geology which comprises of very old rocks that have been subjected to several geological events. These rocks contain several mineral ores which include gold, marble, limestone, kimberlites, lead, iron ore, copper, kaolin and bentonite clays and uranium; these rocks are greatly found in the eastern and south western Uganda. Kapchorwa District is found in Eastern Uganda and is one of the regions endowed with minerals such as gold, limestone, gypsum, marble and granite stones; Limestone occurs in Neogene carbonatite complexes and volcanic rocks found in Eastern and South western Uganda. Data recorded by the Department of Geological Surveys and Mines, between 2002 and 2011 indicated that mineral production and exports increased greatly with limestone, pozzolana and gypsum posting the highest production figures. This was attributed to the high demand of cement in the East African region. (www.uganda-mining.go.ug, 2012).

The major geological activity in Kapchorwa District is limestone quarrying and the main limestone quarry in Kapchorwa District is Kaserem limestone Quarry. This quarry is located in Kawowo sub-county, Kapchorwa District. Quarrying in this place is done in two ways namely: surface excavation of stones, milling into small particles at the site, and at the same time local crude methods are employed by the local inhabitants around the quarry. They use hoes for digging stones, Iron rods and hammers for shaping limestone to brick form and crushing these limestone into hard core for building; since making of bricks is not possible in Kapchorwa District given the nature of the soils. In this area, houses are mainly constructed out of curved stones, mud wattle from soils and cow dung.

Rocks, building materials, water, soil, and the atmosphere contains varying amounts of minerals. All minerals and their raw materials contain radionuclides of natural and terrestrial origin which are commonly referred to as primordial radionuclides (Odumo, 2009). Some of these radionuclides from these sources are transferred to humans through the food chain or inhalation. During the process of milling and extraction of stones, dust rises into the atmosphere and escapes to the community which exposes the inhabitants and miners to dust

which may contain long lived alpha and gamma emitting radionuclides (UNSCEAR, 2000). The inhabitants also depend on water sources in the neighborhood and carry out farming around the quarry. This therefore means that the soil, water bodies, dust and crops could be potential sinks for these radionuclides which will ultimately end in the human body.

Natural radionuclides in soil are responsible for the background radiation exposure to the population. It is estimated that 80% of the collective radiation exposure dose to the world population in the environment is derived from natural radionuclides, while the remaining 20% is from cosmic rays (IAEA, 1996). Gamma radiations emitted from naturally occurring radionuclides are called Terrestrial radiations; These arise from natural radioactive elements present in varying amounts in all types of water, soil, air, rocks and other environmental materials (Alaamer, 2008, Kinyua et al., 2011). According to UNSCEAR (2000) exposure from naturally occurring radioactive materials gives the major contribution to the total effective radiation dose of the population. The exposure pathways of these naturally occurring radionuclides include internal exposure, mainly due to ingestion, inhalation or absorption of radioactive materials and external exposure due to the gamma irradiation with radionuclides originating from primordial radionuclides of the earth's crust (Mose et. al., 1990). Naturally occurring radionuclides, dated back to the earth formation are the major contributors to the external sources of irradiation to human population. Earth's distribution of radionuclides is related to the rocks from which the soils originate and the processes that concentrate them. Higher radiation levels are associated with igneous rocks such as granite while lower radiation levels are associated with sedimentary rocks with exception of shale and phosphate rocks (NCRP, 1993). In addition to the natural background radiation people are exposed to low and high linear energy transfer radiation from "man made" sources such as X-ray equipment and radioactive materials used in medicine, research and industry as shown in Figure 1.1.

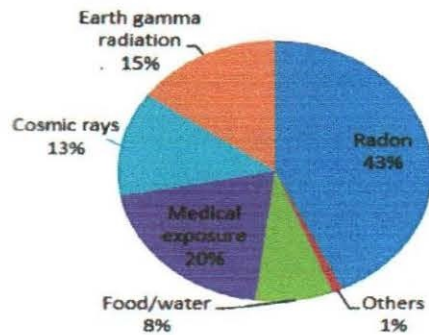


Figure 1.1: A pie chart showing average world percentage of radiation exposure by different sources of radiation (WHO, 2013)

The Figure 1.1, shows the average world percentages of radiation exposure by different sources of radiation with the largest source being “natural radiation” arising from cosmic rays, earth gamma radiation, radon gas which comes from the natural decay of uranium in soil, water and rock while “man made” radiation consists of x-rays used in medicine, agriculture and industry with nuclear weapons testing, nuclear power and some consumer goods.

Exposure to radiation may lead to different health effects. The type and probability of the produced effects generally depend on the radiation dose received, type of radiation and observed end point; the biological effects of radiation exposure include kidney damage, mutagenic leukemia as well as cancer. Thorium exposure can cause lung, pancreas, hepatic, bone, kidney cancers and leukemia (Taskin et al., 2009; Feroz, 2015). Research has shown that cancer is associated with exposure to ionizing radiations of both of natural and artificial origin (Taskin et al., 2009, Feroz, 2015). Ionizing radiation can cause tissue damage, this occurs through the change in chemical properties of molecules in the tissue following exposure. The major contributor to damage from radiation is through radiation changing a water molecule into a new form called free radical. Free radicals are highly chemically active and as such can have reactions with genetic molecules of the cell called the Deoxyribonucleic Acid (DNA). This can cause damage to the DNA and if the DNA damage results into cell death then this is termed as deterministic effect of radiation exposure, while if the DNA encoding leads to other adverse changes then this is termed as stochastic effect of radiation exposure leading to cancer induction (www.imagewisely.org, accessed on 1st July, 2016)

A report by the Uganda Government, Ministry of Health, during a cancer camp in Tororo District, Uganda as presented by Dr Jackson Orema, a cancer expert, based at Uganda Cancer

Institute in Mulago Referral Hospital, indicated that 22,000 new cases of cancer are recorded yearly, and 20,000 also die yearly (www.uci.or.ug, accessed on 16 October, 2015). In a period of three years between 2011 to 2013 the number of cancer patients admitted at the national referral hospital shot up from 1200 to 2800 (Musoke, 2013).

Although, literature shows that studies on specific activity concentration of radionuclides in mines have been done in other countries, such as Egypt, Nigeria, Kenya, Saudi Arabia, Ghana and Tanzania (e.g Darwish & Abdul-Nasr, 2014; Ademola et al., 2014; Kinyua et al., 2011; Najat et al., 2013; Nasiru, 2013; Osoro et al., 2011; Aguko et al., 2013), there seems to be scanty information about the activity concentrations of radionuclides in quarry areas in Uganda. Kinyua et al (2011) carried out a radiological study on the activity concentration of ^{40}K , ^{232}Th and ^{226}Ra and exposure levels in the Tabaka soapstone quarries of Kisii region in Kenya; the findings showed that the activity concentrations of ^{40}K , ^{232}Th and ^{226}Ra Ranged from 38.6 Bq kg^{-1} to 271.7 Bq kg^{-1} for ^{232}Th , 43.1 Bq kg^{-1} to 360 Bq kg^{-1} for ^{226}Ra , and 245 Bq kg^{-1} to 1780 Bq kg^{-1} for ^{40}K . In all the quarries sampled ^{40}K had the highest concentration. The measured absorbed dose rate in air was 541.4 nGy h^{-1} which are 9 times higher than the world measured average and 3 times higher than the calculated average. The mean annual effective dose ranged from 0.215 mSv y^{-1} to 0.875 mSv y^{-1} with a mean of 0.44 mSv y^{-1} which corresponds to an excess lifetime cancer risk of 0.07% and is less than 1 mSv y^{-1} maximum permissible limit recommended for the public by International Commission on Radiation Protection (ICRP). Also the internal and external hazard indices were 1.03 and 1.27 respectively (Kinyua et al., 2011). These values were greater than unity hence slightly exceeding the maximum permissible limits set by the International Commission on Radiation Protection (ICRP).

Darwish et al., (2015) investigated natural radioactivity and its associated radiological hazards and dose parameters in granite samples from South Sinai, Egypt. The results showed that some samples registered values for exposure dose rate higher than the permissible limits but all other parameters were lower as compared to the world average. In Tanzania, Najat et al., (2013) did research on radioactivity from naturally occurring radionuclides (NORM) in soil and water from Likuyu village in the neighborhood of Mkuju Uranium deposit and the findings were that; the average specific activity values of natural occurring radionuclides of ^{238}U , ^{232}Th and ^{40}K were 51.7 Bq kg^{-1} , 36.4 Bq kg^{-1} and 564.3 Bq kg^{-1} respectively for the soil samples. These were higher than the world wide concentrations of the radionuclides

(UNSCEAR, 2000). For water samples the specific activity due to ^{238}U and ^{232}Th were 2.35 Bq l^{-1} and 1.85 Bq l^{-1} respectively. These values were also higher than the world wide average specific activities for water, but were comparable to that obtained for the control samples of water.

1.2. Statement of the Problem

Quarrying as a form of mining, results into large volumes of mine tailings, which may contain enhanced levels of radionuclides. Leaching of these radionuclides, can result in contaminated ground and surface water bodies, thereby exposing members of the public to radiations (Faanu, 2011). Also lack of proper facilities and poor safety culture in mines and quarries can lead to increased radiation exposure and radiological risks for the local artisan miners.

A survey was conducted and data from Kapchorwa District Hospital records revealed that Kapchorwa District registered about seventy (70) cases of cancer, Kween District, thirty (30) cases of cancer, and Bukwo District, twenty (20) cases of cancer. From this data, Kapchorwa District posted the highest number of cancer cases between the years 2011 to 2015 (obtained from Kapchorwa District Hospital records, accessed in January, 2015). Of these seventy (70) cases of cancer registered in Kapchorwa district, the majority of the patients came from Kaserem and Kawowo sub-counties which are areas that surround the quarry. The most common cancer cases registered in this area were Thyroid and Oesophagus cancer; though there are many causes of cancer and some cancers have long latent periods before they manifest. As compared to the other three districts of Sebei sub-region in Eastern Uganda, there is a high number of cancer cases registered in Kapchorwa district, particularly in Kaserem and Kawowo sub-counties. But information regarding the specific activities of natural radionuclides present and their contribution to dose rates in Sebei sub-region is scanty. It's against this background that the researcher has been prompted to carry out the study to determine the natural radioactivity level and radiation hazard indices of the gamma ray emitting radionuclides present in the soils and water from Kaserem limestone quarry area.

1.3. Purpose of the Study

The main purpose of the study was to determine the natural radioactivity levels and radiological hazard indices due to gamma ray emitting radionuclides present in soil and water in Kaserem limestone quarry area

1.4. Objectives of the Study

The Objectives of the study were to:

- i. Determine the specific activities of the gamma ray emitting radionuclides in soils and water from Kaserem limestone quarry area.
- ii. Compute the absorbed dose rate
- iii. Determine the annual effective dose
- iv. Find the radiation hazard indices

1.5. Significance of the Study

Since there is scanty information about specific activity values of gamma emitting radionuclides in mining areas in Uganda, particularly in Sebei sub-region, the present study will be useful in providing data for protecting the public from radiation exposure and minimizing risks associated with exposure in Kaserem Limestone quarry Area. It will also help the relevant authorities and artisan miners to take precautionary measures, to protect the local community against the radiations.

The study will also be important to the Atomic Energy Council of Uganda, the regulatory authority mandated to implement radiation protection standards for the general population in Uganda.

The data generated from this study will also be used as a reference data while conducting further research.

1.6. Scope of the Study

The study only considered Kaserem limestone quarry area in Kapchorwa District in Eastern Uganda. This quarry is located in Kawowo sub-county which was formerly part of Kaserem sub-county and is 4 km from Bulambuli Town Council along Muyembe-Kapchorwa road as shown in Figures 1.2 and 1.3.



Figure 1.2: Google satellite map showing the location of Kaserem Limestone Quarry (source, Google maps accessed on 1st Oct, 2017)

The Global positioning location of the quarry as shown in Figure 1.2 is latitude $1^{\circ}20'35.5''$ N and longitude $34^{\circ}19'02.8''$ E. The research focused only on five locations for soil samples code named A, B, C, D and E as shown in Figure 3.0 and two water sources near the quarry. A total of sixty samples were analyzed in the study; of these, fifty (50) samples were for soil collected from the quarry area and its surroundings and ten (10) water samples picked from the two nearby sources, a stream and protected spring for analysis.

The research was limited to the four specific objectives stated above and it was also time bound i.e. the time frame for carrying out the research was between December 2015 and May 2016.

The challenge that was encountered while carrying out the research was financial difficulty, since the samples were picked from Kapchorwa district and taken to the department of physics laboratory, Makerere University for analysis

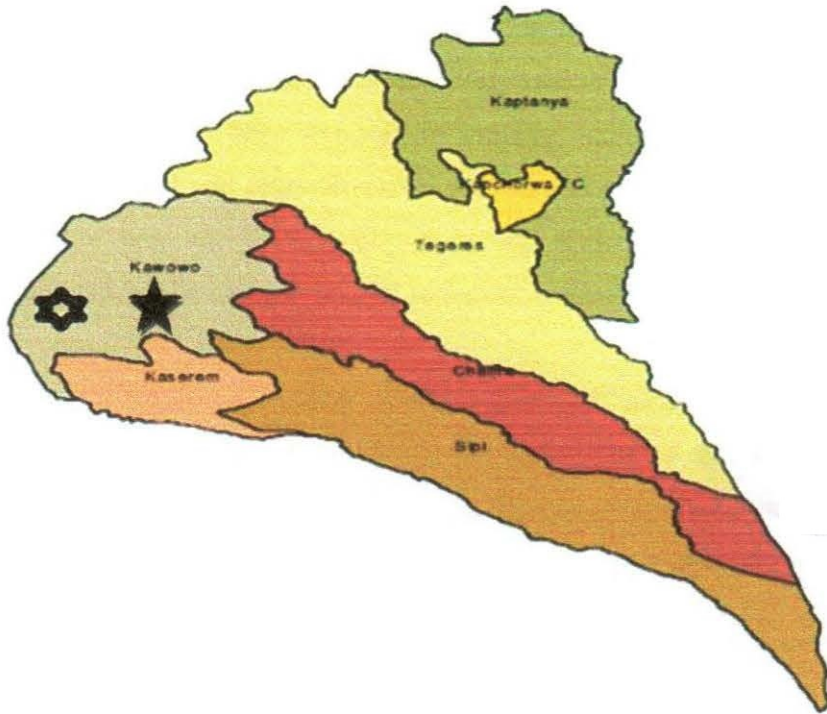


Figure 1.3: Map of Kapchorwa District showing location of the quarry. (www.ucc.co.ug, accessed on 16th October, 2015)

Key: ★ Location of the quarry

CHAPTER TWO: REVIEW OF RELATED LITERATURE

2.1. Introduction

Industrial activities such as oil and gas extraction, coal and peat fired power generation, phosphate industries, zircon/zirconium industry, production of titanium dioxide pigments, mining and processing of metals have been reported as potential sources of elevated values of specific activity due to naturally occurring radionuclides (NORM), (Faanu, 2011). Human beings have always been exposed to ionizing radiations from natural occurring sources; namely terrestrial and extra-terrestrial radiation (Kinyua et al., 2011). Terrestrial radiation is due to the presence of naturally occurring radionuclides (NORM) from the terrestrial environment, while extra-terrestrial radiation originate from high energy cosmic ray particles from space (UNSCEAR, 2000).

This chapter reviews the theory of major aspects of radionuclides and the literature of other researchers whose work is related to the objectives of this study. The concepts that are covered in this chapter include: Types and sources of radiation, process, nature and behaviour, naturally occurring radioactive radionuclides (NORM), radioactivity and biological effects of radiation.

2.2. Types and Sources of Radiation

Radiation in general is concerned with emission of energy by matter in the form of rays or high speed particles (Chege et.al. 2014). Radiation is classified into two main categories namely: non ionizing radiation and ionizing radiation, depending on its ability to ionize. Non ionizing radiation cannot ionize matter when it interacts with it, while ionizing radiation can ionize matter on interaction because the energy of the incoming photon exceeds the ionization potential of matter. Examples of non ionizing radiation are visible light, infrared, radio waves, micro waves and sunlight (Alpen, 1998).

Ionizing radiation falls into two broad groups, particle radiation such as high energy electrons, neutrons, protons and alpha particles that ionize matter by direct atomic collision and electromagnetic radiations or photons such as X-rays or gamma rays which ionize matter by other types of atomic interactions (Busby & Fucic, 2006). The main sources of ionizing

radiations are long lived Uranium, Thorium elements and their decay products and potassium (Tawalbeh et al., 2012). The most primordial radionuclides include ^{40}K radionuclide and the three decay chains which start with radioisotopes of ^{235}U , ^{238}U and ^{232}Th series radionuclides. The decay products of the three radioisotopes of ^{235}U , ^{238}U and ^{232}Th gives rise to chains of radioactive decay products known as decay series. The decay products of these isotopes are part of the natural background (Okeyede & Oluseye, 2010). The instrumental technique used in establishing these radionuclides and gamma ray interaction with matter will be discussed in the sub sections below.

2.3. Gamma-ray interaction with matter

Gamma rays are energetic photons whose wavelengths cover a wide range. After a decay reaction the nucleus is often in an excited state. Rather than emitting another beta or alpha particle this energy is lost by emitting a pulse of electromagnetic radiation called gamma ray. Gamma rays interact with a medium by colliding with electrons in the shells of the atoms, they lose their energy slowly in the medium since they are able to travel significant distances before stopping (Gilmore, 2008; Turner, 2007). Gamma ray interaction takes place in one of the three different ways: photoelectric absorption, pair production and Compton scattering (Alpen, 1997; Cember, 2009). These different interactions change their probability of occurring depending on the energy of the gamma ray and the atomic number (Z) of the material as shown in Figure 2.1.

KYAMBOGO UNIVERSITY
LIBRARY
RARE COLLECTION

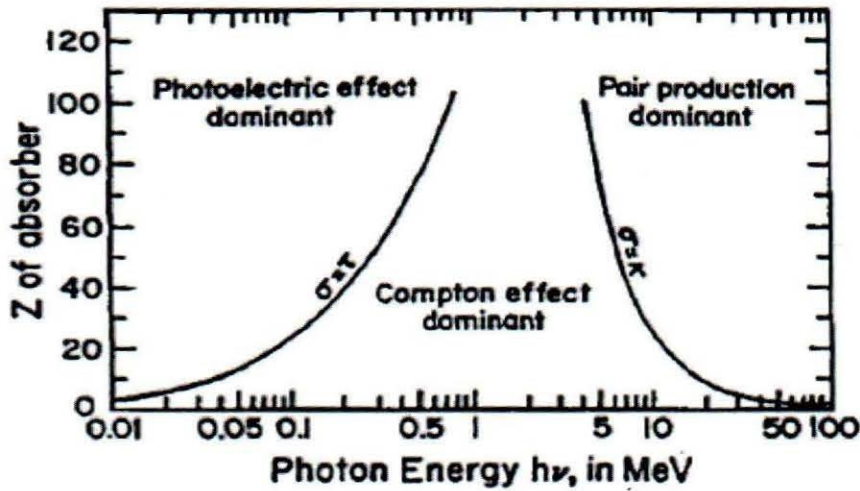


Figure 2.1: A graph depicting the various regions where the different gamma-ray interactions are dominant. (Attix, 1986)

As it can be seen from Figure 2.1, the photoelectric effect is dominant for low energy photons and high Z materials. Pair production is dominant for high energy photons and high Z materials. The Compton scattering interaction is dominant for moderate energies.

In photoelectric effect the photon interacts with a tightly bound orbital electron of an attenuator and disappears while the orbital electron is ejected from the atom as photoelectron. The kinetic energy that this electron carries off is given by (Rittersdorf, 2007; Gilmore, 2008)

$$E_{e^-} = h\nu - E_b \quad (2.1)$$

Where E_b the binding energy of the liberated electron in its original shell and $h\nu$ is the energy of the incoming photon. In this process the photoelectron carries away most of the gamma ray energy and then an X-ray or Auger electron carries away the remaining kinetic energy (Larmarsh, 2012).

Pair production: High-energy gamma rays of 1.022 MeV are absorbed; two particles are created (an electron and a positron) and share the energy of the gamma ray. The electron interacts with matter, as explained above for beta interaction. The positron, losses its energy through ionization or excitation (Rittersdorf, 2007)

Compton Effect: Here the gamma ray interacts with an electron in the absorbing material causing an increase in the electrons energy. Compton scattering is the most predominant

interaction mechanism for gamma ray energies typical of radioisotope source. Incident gamma ray photon is deflected through an angle θ with respect to its original direction and a portion of the energy is transferred to the electron which is known as the recoil electron as shown in Figure 2.2.

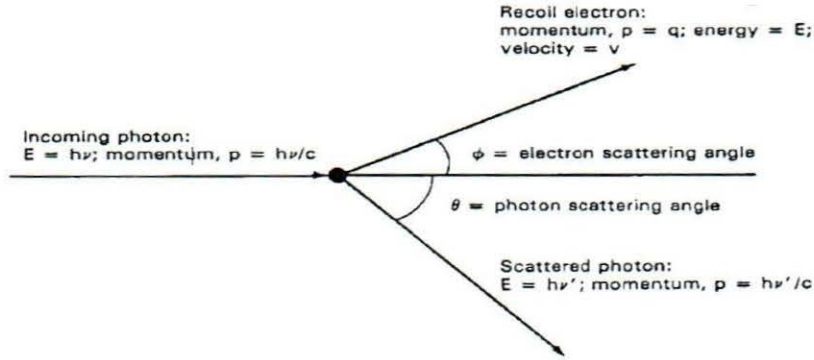


Figure 2.2: Schematic diagram of Compton scattering, Alpen (1998)

Figure 2.2 shows, Compton scattering and here all angles of scattering are possible hence the energy transferred to the electron, can vary from zero to a large fraction of the incident photon energy. The maximum energy that a photon can transfer to an electron is when $\theta = 180^\circ$. The scattering angle between 0° and 180° and the smaller the angle the smaller the amount of energy transferred (Cember, 2009). By writing simultaneous equations for conservation of energy and momentum and using the symbols defined in Figure 2.2.

$$h\nu' = \frac{h\nu}{\left(1 + \frac{h\nu}{m_0c^2}\right)(1 - \cos\theta)} \quad (2.2)$$

The expression in equation 2.2 relates energy transfer and scattering angle for any given interaction. The probability of Compton scattering per atom of the absorber depends on the number of electrons available as scattering targets and thus increases linearly with atomic number Z (Alpen, 1998; Cember, 2009; Turner, 2007).

2.4. Gamma-ray Spectroscopy

Detecting X-rays and gamma rays is not a direct process and in order for gamma rays to be detected it must interact with matter and that interaction must be recorded. Fortunately the electromagnetic nature of gamma ray photons allows them to interact strongly with the charged electrons in the atoms of all matter (Rittersdorf, 2007). Gamma ray spectrometry is an analytical method that allows the identification and quantification of gamma ray emitting isotopes or radioisotopes by measuring the energy distribution of the source. A spectrometer is an instrument that separates the output pulses from a detector, usually a scintillation detector or a semi conductor according to size of radionuclide distribution. Since the size of radionuclide distribution is proportional to the energy of the detected radiation, the output of the spectrometer provides detailed information that is useful in identifying radioisotopes and counting one isotope in the presence of others (Cember, 2009).

The process of radiation detection by a semi conductor can be explained by the characteristic of a single crystal of a semiconducting material in terms of the band structure. They have two distinct energy bands, which are a valence band and a conduction band. The valence band, which is the lowest energy band, consists of the outer electrons bound to specific lattice sites within the crystal, whereas, the conduction band, which is the higher energy band, contains electrons that can move through the crystal. When the electrons in the valence band of a semiconductor are thermally excited, they are able to jump across the forbidden region to the conduction region and this forms the basis of the semiconductor gamma-ray detector (Atambo, 2011; Turner, 2007).

Figure 2.3, shows a scintillator employed in radiation detections.

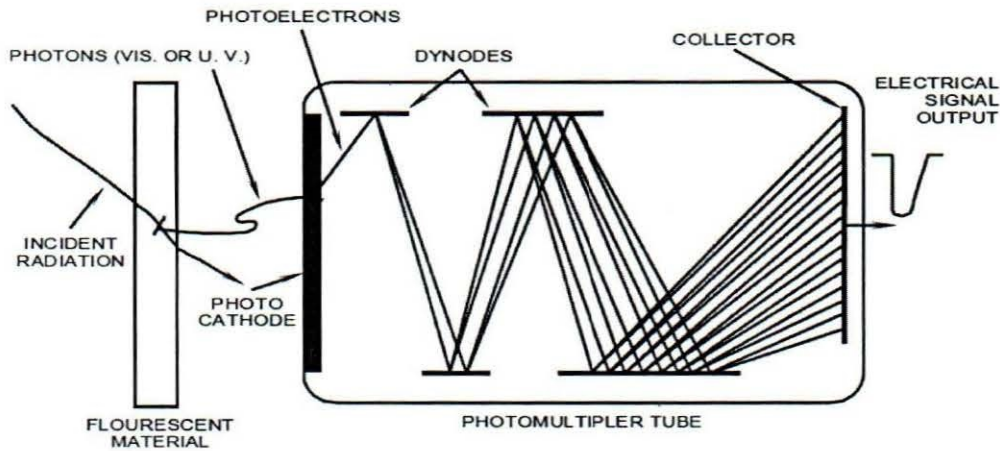


Figure 2.3: Structure of Scintillator detector, Mattetnik(1995)

They are usually surrounded by reflecting surfaces to trap as much light as possible. The light is fed into a photomultiplier tube for generation of an electrical signal; then a photosensitive cathode converts a fraction of the photoelectrons which are accelerated through an electric field towards another electrode called a dynode. In striking the dynode each electron ejects a number of secondary electrons, giving rise to electron multiplication. This gives rise to a final signal which is proportional to the scintillator light output and under right conditions is proportional to the energy loss that has produced the scintillation (Turner, 2007).

The two main types of scintillator detectors for gamma-rays are: germanium semiconductor detectors and inorganic Scintillators such as NaI(Tl). Inorganic Scintillators particularly Sodium Iodide Thallium detector, NaI(Tl) will be described here since it is the instrument that was used for measurement as shown in Figure 2.4.

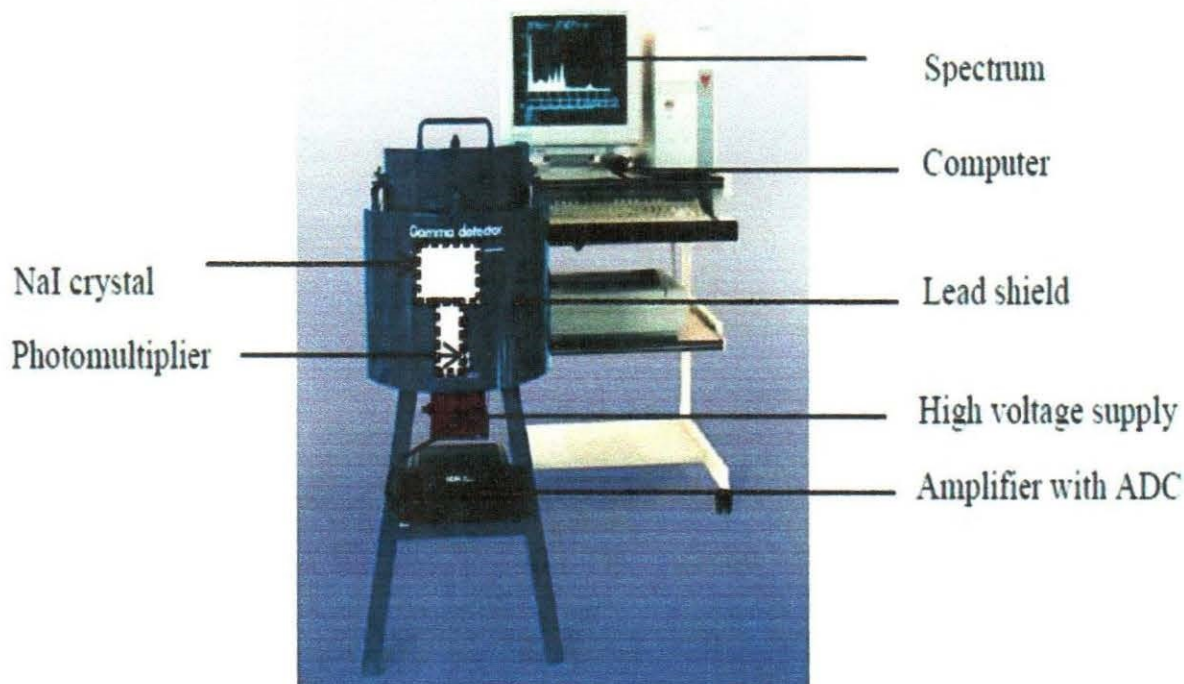


Figure 2.4: Spectrometer system for nuclear radiation (www.gammadata.net)

Sodium Iodide Thallium detector, NaI(Tl), is optically coupled to a photomultiplier tube. When a gamma ray enters the detector, it interacts by causing ionization of sodium iodide. This creates excited states in the crystal that decays by emitting visible light photons a process called scintillation. The thallium doping of a crystal is done to shift the wavelength of the light photons into the sensitive range of the photocathode. It converts the energy absorbed in the crystal to light. The high density and its high effective atomic number, results in high detection efficiency (Cember, 2009). A typical Sodium iodide thallium detector, NaI(Tl) is shown in Figure 2.4 Gamma-ray spectrometers are available in two types either a single channel instrument or a multichannel analyzer (MCA). The essentials parts of a single channel analyzer are shown in Figure 2.5.

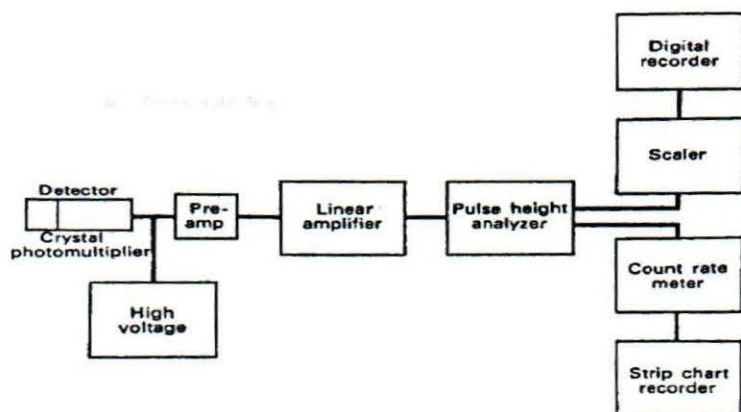


Figure 2.5: Block diagram of a single channel analyzer, Cember (2009)

It consists of a detector, a linear amplifier, a pulse height selector and a readout device such as the scale or rate meter. The pulse height selector is an electronic slit which may be adjusted to pass pulses whose amplitude lies between two desired limits, minimum and maximum output. The main use of this analyzer is to discriminate between a desired radiation and the other that may be considered as noise (Cember, 2009).

A multichannel analyzer (MCA), has an analog to digital converter (ADC) instead of a pulse height selector, to sort all the output pulses from the detector according to height. The MCA also has a computer memory for sorting the information from the ADC or from another source as shown in Figure 2.6.

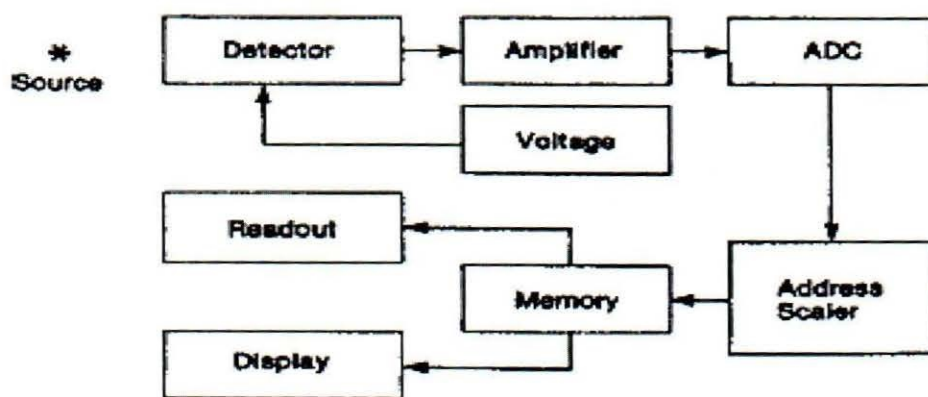


Figure 2.6: Block diagram showing a multichannel analyzer MCA, Cember (2009)

This feature allows automated data processing operations such as background subtraction and stripping. Spectrum stripping is a technique for analysis of compound spectra that is based on sequential subtraction of known gamma-ray spectra of individual isotopes from the compound spectra.

2.5. Activity concentration of gamma ray emitting radionuclides

Naturally occurring radionuclide materials existed since the creation of the earth (UNSCEAR, 2000). Many of the radionuclides were radioactive and have decayed away. A few of these radionuclides have half-lives longer than or comparable to the age of the earth (Kinyua et al., 2011), and they are still in existence. The gamma radiation emitted from these radionuclides gives to human beings a radiation dose. Radioactivity and radioactive decay are discussed in the following sub sections.

Radioactivity: This is a spontaneous nuclear transformation of an unstable atoms (parent) resulting into the formation of new elements (daughter). The unstable nucleus may transform into a more stable configuration and emit excess energy in the form of radiation. (Krane,1987). There are three primary decay types of radiation emitted by radioactive substances; these are alpha particle emission, beta and gamma decays. In alpha and beta decay processes an unstable nucleus emits alpha and beta particles to become a stable nucleus, whereas in gamma decay process a nucleus in an excited state decays towards a lower energy state without changing the nuclear species (Lilley, 2002; Cember, 2009). A radioactive decay can lead to emission of one or more photons from the excited states of daughter nuclei in the form of alpha, beta or gamma particles. Transitions that results in gamma emission leave Z and A unchanged and are called isomers (Turner, 2007)

Alpha decay: Alpha particles can interact with either nuclei or orbital electrons in any absorbing medium. This may be deflected with no change in energy or with a small change in energy.

During alpha particle decay, a highly energetic helium nucleus is emitted from the nucleus of an unstable atom. This takes place when the neutron to proton ratio is too low (Cember,

2009). When a nucleus undergoes alpha decay there is a reduction in both the mass and charge on the final nucleus (Krane, 1987) i.e.



From the law of conservation of energy and momentum (Cember, 2009); the energy Q released during the decay process is given by

$$Q = (M_P - M_D - M_\alpha)C^2 \quad (2.4)$$

And writing the equation above in terms of E , the kinetic energy of the alpha particles, we shall have

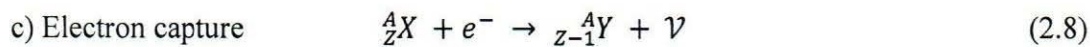
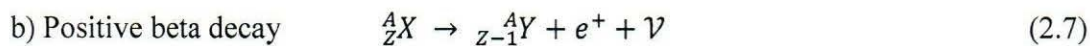
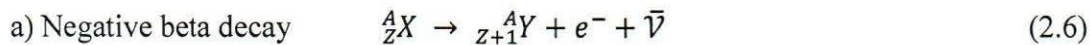
$$Q = E\left(\frac{M_\alpha}{M_D} + 1\right) \quad (2.5)$$

Where m_p , m_D and m_α are the masses of parent, daughter and alpha particles respectively.

Beta decay: Beta particles can interact with electrons as well as nuclei in the medium through which they are travelling. They are deflected by coulombs forces in the medium resulting into ionization. In beta decay an electron is ejected from the nucleus of an unstable radioactive atom whose neutron to proton ratio is too high (Cember, 2009; Turner, 2007)

Beta particles can be either a negatron or positron. It is a negatron if the electron has a negative charge (β^-) and when emitted, the nucleus charge rises by 1 whereas it is a positron if it has a positive charge (β^+) and when emitted, the nucleus charge decreases by 1 (Lilley,2002)

The three processes under beta decay are illustrated by the equations below



Where ν , $\bar{\nu}$ and e^- are the neutrino, antineutrino and an electron.

In the process of electron capture, an electron in the K-shell interacts with one of the protons in the nucleus and a neutron is consequently formed (Cember, 2009).

Gamma decay: Gamma rays are electromagnetic radiations emitted from the nuclei of excited atoms following radioactive transformations (Gilmore, 2008; Cember, 2009). These transformations are characterized by one of the several mechanisms including alpha particle, beta particle emission, positron emission, and orbital electron capture (Cember, 1996; lilley, 2002). If the daughter is an unstable nucleus, the decay process continues until the end daughter is reached to a stable nucleus; this process occurs in a random way and nobody can know exactly when unstable nucleus will decay. The probability per unit time can be specified just to know when the unstable nucleus will decay over time. This is normally described by the half life, which is the time taken for half the nucleus in the sample to decay (lilley, 2002). The decay probability is the fundamental property of an atomic nucleus and remains equal at all time (Flurry, 2006; L'Annunziata, 2007). Mathematically, the law can be expressed as

$$\frac{dN}{dt} = -\lambda N \quad (2.9)$$

Where λ is the decay constant (disintegration constant), N the number of radioactive atoms of a given source at a given time, t . The solution of equation (2.9) above leads to the exponential law of radioactive decay as given by (Krane, 1987).

$$N = N_0 e^{-\lambda t} \quad (2.10)$$

Where N_0 is the original number of nuclei present at $t=0$.

The half life, $t_{\frac{1}{2}}$, is the time for half of the nuclei to decay.

The value, $N = \frac{N_0}{2}$, When time $t = t_{\frac{1}{2}}$, the equation (2.10) gives (Krane, 1987)

$$t_{\frac{1}{2}} = \frac{\ln 2}{\lambda} = \frac{0.693}{\lambda} \quad (2.11)$$

The strength of radioactivity is called activity (A). Activity (A) is defined as the number of disintegrations of an atom per unit time (L'Annunziata, 2007)

$$A = \frac{dN}{dt} = -\lambda N \quad (2.12)$$

Radioactive Decay series: The series occurs when a parent nuclei decays to a daughter product which is also radioactive (Krane, 1987; Turner, 2007; L'Annunziata, 2007). Consider a radioactive decay which begins with a radioactive parent nucleus, P , with decay constant, λ_p into a daughter, D with decay constant, λ_d and finally into a stable grand-daughter G i.e.



It follows that the number of P , D and G at a time, t will be given by the equations(2.15&2.16) (L'Annunziata, 2007). At any time t , the activity of the parent is, $\lambda_p N_p$, and the activity of the daughter is $\lambda_d N_d$ where N_p , N_d and N_G are the number of atoms of the parent P , daughter D and grand-daughter, G , at time t , are given by (Alpen, 1998)

$$\frac{dN_p}{dt} = -\lambda_p N_p ,$$

and

$$\frac{dN_d}{dt} = \lambda_p N_p - \lambda_d N_d . \quad (2.14)$$

Equation (2.14) represents the activity found for the daughter at any time which is equal to the initial amount corrected for its decay ($-\lambda_d N_d$) plus the new daughter activity produced by the decay of the parent ($\lambda_p N_p$), (Alpen, 1998)

Integrating equation (2.9) yields a solution for the number of atoms of the daughter N_d , at any time t , as given by (Alpen, 1998)

$$N_d(t) = N_p(t_0) \frac{\lambda_p}{\lambda_d - \lambda_p} (e^{-\lambda_p t} - e^{-\lambda_d t}) + N_d(t_0) e^{-\lambda_d t}. \quad (2.15)$$

The special case for the applications of equation (2.15) is that the starting activity of the daughter nuclide is zero; that is, there has just been a chemical separation of the daughter from the parent and in this case the last term disappears (Alpen, 1998; Turner, 2007)

$$N_d(t) = N_p(t_0) \frac{\lambda_p}{\lambda_d - \lambda_p} (e^{-\lambda_p t} - e^{-\lambda_d t}) \quad (2.16)$$

If the grand-daughter G of the radioactive decay is still unstable, then this process continues until another stable product is formed. This implies that it is possible to have a series of decay chains (Turner, 2007), and this is called radioactive equilibrium

Radioactive Equilibrium: This is used to describe the condition when the activity of each radionuclide decays at the same rate with which it is produced (Krane, 1987; Turner, 2007). There are three general cases of the state of equilibrium which include: secular equilibrium, transient equilibrium and no equilibrium.

Secular equilibrium occurs when a long-lived parent (P) decays into a relatively short-lived daughter (D) which in turn decays into a stable nuclide. From equation (2.16), if $T_P \gg T_d$, then, $\lambda_p \ll \lambda_d$ and $N_d(0) = 0$, the general equation yields (Alpen, 1998)

$$N_d(t) = N_P(0) \frac{\lambda_p}{\lambda_d} (1 - e^{-\lambda_d t}) . \quad (2.17)$$

As time increases $e^{-\lambda_d t}$ will tend to zero, hence equation (2.17) reduces to

$$\lambda_d N_d = \lambda_p N_p . \quad (2.18)$$

where the λ_p and, λ_d are the decay constants of the parent and daughter nuclei respectively. Here the activity of the parent is equal to the activity of the daughter.

Transient equilibrium occurs when the half life of the parent is greater than that of the daughter but not so greatly, $T_P \geq T_d$, and that, $\lambda_p < \lambda_d$. As time passes $e^{-\lambda_d t} \approx 0$, and equation (2.16) reduces to

$$N_D(t) = N_P(0) \frac{\lambda_p}{\lambda_d - \lambda_p} e^{-\lambda_p t} \quad (2.19)$$

Since, $N_p(t) = N_P(0) e^{-\lambda_p t}$ in equation (2.18) can be expressed as

$$N_D(t) = N_P(t) \frac{\lambda_p}{\lambda_D - \lambda_P} . \quad (2.20)$$

Thus after initially increasing, the daughter activity goes through a maximum and then decreases at the same rate as the parent activity (Turner, 2007)

No equilibrium occurs when the daughter, initially absent has a longer half life than the parent $T_p < T_D$, its activity builds up to a maximum and then declines (Turner, 2007)

2.6 Biological Effects of Radiation

When a human body is exposed to radiation either from external or internal sources, ionization and excitation of atoms and molecules can be produced. Since body cells consist of water, H_2O . When a H_2O molecule is struck by ionization radiation, the molecule picks up the energy lost by the radiation in the collision. If the energy gain is sufficient to overcome the bonding force holding the molecule together, the molecule will break up as shown in equation (2.21):



These two ions produced from an H_2O molecule are known as “free radicals”



From equation 2.22 above, radiation interacts with free cellular water to produce one free electron (e^-) and one ionized water molecule (H_2O^+), a reaction commonly known as radiolysis. This free electron is highly reactive and interacts with another un-ionized water molecule to produce a negatively charged and highly unstable water molecule. This molecule quickly decomposes to form the OH^- ion and the H^\bullet free radical; the H^\bullet radical is reactive, but the OH^- ion is more stable and can then diffuse out into the cellular fluid and interact with any number of macromolecules it encounters in its path, such as molecules of DNA. The remaining H_2O^+ molecule can also transform into a free and ionized hydrogen ion (potentially affecting intracellular or extracellular pH) and the hydroxyl radical. From these reactions, four products of radiolysis can occur after ionizing radiation interacts with a water molecule: H^\bullet , OH^\bullet , H^+ , and OH^- (Kuhn, 2003)

The most important consequence of this displaced electron on human tissue is the potential damage it can inflict on Deoxyribonucleic acid (DNA) which may occur directly or indirectly. Direct damage occurs when the displaced electron hits and breaks a DNA strand while indirect damage occurs when the electron reacts with a water molecule creating a powerful hydroxyl radical which then damages the DNA cells (Goodman, 2010; Alpen, 1990). If the

damage to the DNA is minor DNA has capability to repair this damage but if the damage cannot be repaired or is not repaired correctly, harmful effects may occur such as cancer, mutations (Goodman, 2010; Cathy & Linda, 2009).

Generally, biological effects of radiation fall into two categories: deterministic effects and stochastic effects. Deterministic effects result from exposure to very large doses of radiation. These effects have a threshold dose and their severity increases with increasing dose. Examples are the acute radiation syndromes that have a threshold in the range of 1–2 Gy, whole-body X-ray or gamma radiation, skin burns in the range of 2–3 Gy, and skin ulceration in the range of 20 Gy. The lower dose for whole-body X-ray or gamma radiation is believed to lie in the range of 3–4 Gy (Cember, 2009).

Stochastic effects occur by chance and are seen in unexposed individuals as well as in exposed individuals and therefore are not unequivocally associated with a radiation exposure. Stochastic effects include cancer and genetic mutations (Badhan, 2012). Exposure to radiation increases the probability of a stochastic effect, and this probability increases with increasing dose (Goodman, 2010). Whereas increased incidence of cancer has been documented among certain heavily exposed populations such as the early radiologists, atomic bomb survivors, and patients who had received radiotherapy, no increased incidence of heritable changes has ever been observed among any human population exposed at any dose (Goodman, 2010; Cember, 2009; Sterba, 2014).

The stochastic effects, either in humans or in animals that have been observed are no different in kind from those observed in unirradiated populations. The difference lies only in the frequency of occurrence. Thus, it is impossible for even the most highly skilled pathologist to definitely attribute any cancer in an exposed individual to the exposure. The only thing that can be done is to estimate the probability based on the patient's exposure history that the cancer can be attributed to the radiation exposure (Cember, 2009).

2.7 Evaluation of Absorbed dose and Annual Effective dose

The exposure to ionizing radiation from natural sources is continuous and an unavoidable feature of life on earth. The major sources responsible for this exposure are due to the naturally occurring radionuclides in the earth's crust (UNSCEAR, 2000). To determine how much of the radionuclides are inhaled and ingested, radiological assessment is in terms of Radium equivalent activity, Absorbed dose rate, and the Annual effective dose rate. The

absorbed gamma dose rates (D) in air at 1m above the ground surface for the uniform distribution of the radionuclides are computed on the basis of the guidelines provided by (UNSCEAR, 1993 & 2000). Absorbed dose rates in air are in nGy h^{-1} and are computed from equation (2.23)

$$D = (0.427C_{Ra} + 0.662C_{Th} + 0.043C_K) \text{ nGy h}^{-1} \quad (2.23)$$

where, C_{Ra} , C_{Th} , and C_K are the activity concentration of ^{226}Ra , ^{232}Th and ^{40}K in Bq kg^{-1} in soil respectively, the values 0.427, 0.662 and 0.043 are the dose conversion factors for converting activity concentration of ^{226}Ra , ^{232}Th and ^{40}K in nGy h^{-1} per Bq kg^{-1} as given in UNSCEAR (2000).

To estimate the annual effective dose rates (AED), the conversion coefficient from absorbed dose in air to effective dose (0.7SvG h^{-1}) and outdoor occupancy factor of (0.2) proposed in UNSCEAR (2000) are used. These values were estimated and used mostly for data from Europe based on the fact in Europe people spent most of their time indoors. In Kenya, the average time spent indoor and outdoor called occupancy factors were 0.6 and 0.4 respectively. (Kinyua et al., 2011; Mustapha, 1999). In Uganda, about 82% of the labour force is majorly rural (UBOS, 2013). The average time spent on economic and care labour activities per week by the rural dwellers is 55 hours (about 7.86 hours per day) which translates to 33% (UBOS, 2013). Therefore, the average outdoor and indoor occupancy factors for the rural community in Uganda are 0.33 and 0.67 respectively (Turyahabwa et al., 2016).

$$\text{AED} = D \times 8760 \text{ h y}^{-1} \times 0.33 \times 0.7 \text{ SvG h}^{-1} \times 10^{-6} \quad (2.24)$$

2.8. Evaluation of radiation hazard indices

The radiation hazards associated with radionuclides is determined by computing the

Radium equivalent activity, which is a weighted sum of activities of ^{226}Ra , ^{232}Th and ^{40}K ; this was calculated using the equation (2.25) below based on the assumption that: 370 Bq kg^{-1} of ^{226}Ra , 259 Bq kg^{-1} of ^{232}Th and 4810 Bq kg^{-1} of ^{40}K produce the same gamma radiation dose rate (Beretka et al., 1985; Alaamer, 2008).

$$Ra_{eq} = C_{Ra} + 1.43 C_{Th} + 0.077 C_K \quad (2.25)$$

where, C_{Ra} , C_{Th} , and C_K are the activity concentration of ^{226}Ra , ^{232}Th and ^{40}K in Bq kg^{-1} respectively. To avoid radiation hazard, materials whose Ra_{eq} is greater than 370 Bq kg^{-1} should not be used. (Alaamer, 2008)

The Internal Hazard Index, H_{in} was calculated using the equation (2.26) (Kinyua et al., 2011; UNSCEAR, 2000; Girigisu et al., 2013).

$$H_{in} = \frac{C_{Ra}}{185} + \frac{C_{Th}}{259} + \frac{C_K}{4810} \quad (2.26)$$

The external hazard due to radionuclide ^{226}Ra , ^{232}Th and ^{40}K is defined in terms of external hazard index or outdoor radiation hazard index, H_{ex} and is calculated by the equation (Beretka, 1985)

$$H_{ex} = \frac{C_{Ra}}{370} + \frac{C_{Th}}{259} + \frac{C_K}{4810} \quad (2.27)$$

Where, C_{Ra} , C_{Th} , and C_K are the activity concentration of ^{226}Ra , ^{232}Th and ^{40}K in Bq kg^{-1} respectively. The value of these indices should be less than 1 mSv yr^{-1} in order for the radiation hazard to be considered acceptable to the public.

2.9 Related studies on natural radioactivity

There are several studies that have been carried out to assess the dangers of human exposure to radiations from naturally occurring radionuclides in the environment. In Saudi Arabia, Alaamer A.S (2008). Carried out, an assessment of human exposures to natural sources of radiation in soil of Riyadh. Activity concentrations were measured by means of high resolution gamma-ray spectroscopy, the specific activity concentration of ^{226}Ra , ^{232}Th and ^{40}K were $14.5 \pm 3.9 \text{ Bqkg}^{-1}$, $11.2 \pm 3.9 \text{ Bqkg}^{-1}$, and $22.5 \pm 63 \text{ Bqkg}^{-1}$ respectively. The mean values of radium equivalent, air absorbed gamma radiation dose rate, annual effective radiation dose and external radiation hazard index were 47.8 Bqkg^{-1} , 23.3 nGy h^{-1} , 0.14 mSv y^{-1} and 0.13 Bqkg^{-1} respectively. These values obtained did not pose any immediate radiological hazard to the population.

Ali et al.,(2012). assessed the radiological hazard of NORM in Margalla Hills limestone in Pakistan, the findings were that the specific activity of the radionuclides ^{226}Ra , ^{232}Th and ^{40}K were $14.32 \pm 0.24 \text{ Bqkg}^{-1}$, $2.05 \pm 0.04 \text{ Bqkg}^{-1}$, and $13.80 \pm 0.20 \text{ Bqkg}^{-1}$ respectively.

The values of the gamma radiation absorbed dose rate, annual effective dose rate and the hazard indices were all very low. The conclusion was that margalla hills limestone does not pose any excessive radiological hazard as a building material and industrial use for common man.

Saad M.H (2014). Carried out an evaluation of natural radioactivity in different regions of Sudan, he found out that the radioactivity concentrations are normal in Northern and the middle of Sudan with an average absorbed dose rate of $40.187 \text{ nGy h}^{-1}$, but the highest radioactivity concentration and dose rate in air was found in southern Sudan with an average dose rate of $120.355 \text{ nGy h}^{-1}$. This value is two times greater than the world average level while the concentrations of radionuclide ^{232}Th , ^{238}U , and ^{40}K were 53.66 Bqkg^{-1} , 31.05 Bqkg^{-1} , and $1157.55 \text{ Bqkg}^{-1}$ respectively. This high dose rate was attributed to high background radiation.

In Kenya, Osoro M.K (2011) carried out radioactivity measurements in surface soils around Maumba and Nguluku villages, the proposed site for Titanium mining project using a HPGe gamma spectrometer. The activity concentrations for ^{226}Ra , ^{232}Th and ^{40}K were, $20.9 \pm 7.6 \text{ Bqkg}^{-1}$, $27.6 \pm 9.1 \text{ Bqkg}^{-1}$, and $69.5 \pm 16.5 \text{ Bqkg}^{-1}$, the absorbed dose rate in air, calculated on the basis of the measured activity concentrations range from 9.8 to 50.0 nGy h^{-1} with an average of 29.2 nGy h^{-1} . The values were well below the world average values stated in table 4.9. Studies on exposure to various components of the natural background radiation in Kenya have been reported by Mustapha (1999). The terrestrial gamma radiation contribution to the total effective dose was reported to be ranging from 0.1 to 2.0 mSv y^{-1} , from cosmic radiations; 0.2 to 0.7 mSv y^{-1} and per capita of 0.40 mSv y^{-1} ; 0.4 to 6.0 mSv y^{-1} from inhalation of radon. It was also reported that radon concentrations ranged from 5 to 1200 Bq m^{-3} in indoor air and from 1 to 410 Bq l^{-1} . The study concluded that the average Annual effective dose in Kenya is higher than the global average basing on the living habits of the people, the relief and the geology of Kenya.

A study in majingu phosphate mine in Tanzania found high concentration of ^{226}Ra in phosphate rock, $5760 \pm 107 \text{ Bq kg}^{-1}$ and waste rock $4250 \pm 98 \text{ Bq kg}^{-1}$ while the surface water had an activity of $4.7 \pm 0.4 \text{ Bq l}^{-1}$ (Banzi et al., 1999).

A study conducted in Nigeria by Ademola (2014) on the activity concentration of natural radionuclides ^{238}U , ^{232}Th and ^{40}K . In soil samples from Itaganmodi gold mining area using

sodium iodide detector showed that the activity concentration of ^{238}U , ^{232}Th and ^{40}K , were $55.3 \pm 1.2 \text{ Bq kg}^{-1}$, $26.4 \pm 2.7 \text{ Bq kg}^{-1}$ and $505.1 \pm 7.1 \text{ Bq kg}^{-1}$ respectively which were higher than the world wide average values (UNSCEAR, 2000). The mean effective dose in the study was 16% higher when compared to the world average value. A similar study carried out in Saudi Arabia, to find out concentrations of natural radioactivity contribution to the absorbed dose from water samples from western province showed that most of the estimated annual dose from samples exceeded the annual limit of the dose allowed by WHO (0.1mSv/y) for all radionuclides in drinking water (Hamidalddin et al., 2011). Also in Tanzania, Mohammad & Mazungu (2013) investigated natural radioactivity in soil and water from Likuyu village in the neighbourhood of Mkuju Uranium deposit using low level gamma spectroscopy. The results showed that the average concentrations obtained in soil samples for the radionuclides ^{238}U , ^{232}Th and ^{40}K were: 51.7 Bq kg^{-1} , 36.4 Bq kg^{-1} and 564.3 Bq kg^{-1} respectively were higher than the world wide concentration value of these radionuclides as reported in (UNSCEAR, 2000) while for water samples the average concentration value of ^{238}U was 2.35 Bq l^{-1} and for ^{232}Th was 1.85 Bq l^{-1} which were comparable to the world average values

In Uganda, Biira (2014), conducted a research on the concentration levels of radon in mines, industries and dwellings in selected areas of Tororo and Busia Eastern Uganda. Results showed that the concentration levels ranged from 28 ± 1 to $97 \pm 5 \text{ Bq m}^{-3}$ and the effective dose varied from $0.71 \pm 0.03 \text{ mSv y}^{-1}$ to $2.44 \pm 0.13 \text{ mSv y}^{-1}$ respectively. Overall these values were all below the world health recommended values and hence Radon concentration in these areas was still within the recommended values.

Anguma (1999) determined the activity levels of cesium in Lake Victoria and Lake Kyoga and the naturally occurring radionuclides in their biota. The study established that there was no cesium in lakes and that all fish species contained measurable levels of radionuclides. Water hyacinth was found to retain significant amounts of potassium while Uranium and Thorium were measurable. This study did not explicitly investigate the specific activity levels of radionuclides in the natural water bodies in the country and their associated hazard levels.

Mugaiga et al., (2016) conducted a research study in Eastern Uganda on radioactivity levels and dose rates from rocks in selected mining areas and quarries, using Sodium Iodide Thallium detector and the results showed that the specific activities of ^{238}U , ^{232}Th and ^{40}K

ranged from $13.95 \pm 0.31 \text{ Bq kg}^{-1}$ to $698.02 \pm 3.38 \text{ Bq kg}^{-1}$ for ^{238}U , $98.68 \pm 1.30 \text{ Bq kg}^{-1}$ to $2397.78 \pm 19.64 \text{ Bq kg}^{-1}$ for ^{232}Th , and $45.97 \pm 2.48 \text{ Bq kg}^{-1}$ to $2183.80 \pm 17.89 \text{ Bq kg}^{-1}$ for ^{40}K . The absorbed dose rates were calculated and the values obtained for all the sites are all above the maximum permissible value of 59 nGy h^{-1} while the annual effective dose rate outdoor for all the sites ranged from 0.30 to 1.37 mSv y^{-1} which suggests a health risk to the inhabitants of some of the areas. Another study was also conducted by Turyahabwa et al.,(2016) in southwestern Uganda on determination of natural radioactivity levels due to mine tailings from selected mines using Sodium Iodide Thallium detector and the results showed that the specific activities of ^{238}U , ^{232}Th and ^{40}K ranged from 35.5 Bq kg^{-1} to 147.0 Bq kg^{-1} for ^{238}U , 119.3 Bq kg^{-1} to 376.7 Bq kg^{-1} for ^{232}Th , and 141.0 Bq kg^{-1} to $1658.5 \text{ Bq kg}^{-1}$ for ^{40}K . The mean absorbed dose rates for Mashonga Gold mine, Kikagati Tin Mine and Butare Iron Mine were calculated and the values obtained for all the sites are $181.2 \pm 66.8 \text{ nGy h}^{-1}$, $167.2 \pm 43.0 \text{ nGy h}^{-1}$ and $191.6 \pm 29.6 \text{ nGy h}^{-1}$ respectively which are more than three times the maximum permissible value of 59 nGy h^{-1} while the mean outdoor annual effective dose rates for three mines were $0.37 \pm 0.14 \text{ mSv y}^{-1}$, $0.34 \pm 0.09 \text{ mSv y}^{-1}$ and $0.39 \pm 0.09 \text{ mSv y}^{-1}$ respectively which are more than five times the world average value of 0.07 mSv y^{-1} . Thus the mine tailings (soil) from these areas must not be used as a major building material to minimize radiological hazards

CHAPTER THREE: RESEARCH METHODOLOGY

3.1 Introduction

The focus of this chapter was to determine the radiation exposure levels due to gamma emitting radionuclides. The chapter will be divided in the following sub sections; research design, sampling and sampling techniques, measurement of activity levels, determination of radiological levels, and presentation of results and analysis of data are discussed in detail in the following sections.

3.2 Design of the study

The research was concerned with determining the activity of radionuclides, their associated hazard indices and there after relate it with work done by other people in Uganda and other countries. The results were also compared with the world tolerable values as stated in UNSCEAR, (2000). Kaserem limestone quarry was chosen based on the number of people from this area who were suffering from cancer. A survey conducted in Kapchorwa district hospital by checking through the medical records of patients who had visited the hospital seeking treatment of cancer, records revealed that this area had a big number of patients suffering from oesophogus cancer. Another survey was done by picking four soil samples from the site, these samples were picked from two locations; one which had heaped debris of excavated soil and the other location where the samples were freshly dug from the ground of undisturbed soil location. This was carried out at the beginning of January, 2016, before the commencement of the whole experiment. This was done to establish the relationship between the specific activities of soils that had stayed for a long period and those that were freshly dug undisturbed soil location at the quarry. It was found out that the values of the specific activities from the two locations were very close implying that there was no significant difference in specific activities.

The number of water sources available was also established and it was found that there were two water sources that exist near the quarry, a stream and a protected spring (i.e underground piped water) which were considered for sampling. In this research soil fresh from underground holes in the quarry and its surrounding location was considered for study.

3.3. Sampling and sampling techniques

The sampling was done in Kaserem limestone quarry in Kapchorwa district. The sampling strategy that was adopted for the soil samples was random, and at each sampling point soil samples were taken from different sections of the area. The sections of the area are as shown in Figure 3.0, three soil samples were collected at the points A, B, C, D and E. This procedure was repeated in all through the quarry following the North, East, South and West direction as indicated by Figure 3.0. For each location like A, ten samples were then randomly chosen for analysis. These samples (about 1kg each) were put into plastic bags, labeled, then double packed and put in a box whose background radiation could be measured using an identifier and transported to the laboratory for analysis. The quarry was divided into four portions as shown in Figure 3.0.

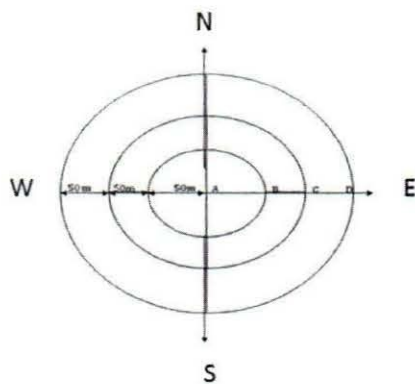


Figure 3.0: A Schematic illustration of how the samples were collected

All the sites were within the quarry and outside the quarry where location A - was the central part of the quarry, B -was at a radius of 50m from A, C at a radius of 100m from A, D at a radius of 150m from A and E was at a distance of 600m from the centre A. The selection of the sample locations was based on the accessibility to the public and also to help identify the trend of levels of activity as we move away from the quarry to the living and farming areas.

Each soil sample was collected from a cluster site at a depth of about 20cm to 30cm using a hand held auger which had been pre cleaned using Nitric acid. The locations were identified using a GPS locator (Global Positioning System), and a total of 50 samples was chosen from this site.

Ten (10) water samples were collected from two water sources at the surrounding to the quarry, a stream and a protected spring. From each water source, five samples (5) were collected. The samples were filled in a one litre acid precleaned plastic containers to avoid wall absorption (IAEA, 1989); and was wrapped using an insulation tape to avoid spill over during transportation of the samples to the laboratory from the sampling site.

3.5 Sample preparation

After collection, the soil samples were dried in an oven at 100°C - 110°C for 24 hours to remove all the moisture and then crushed separately into powder form to homogenize; this is done to increase the efficiency of detection by GDM-20. The powder was then sieved through 2mm mesh and each prepared sample was stored in a 500ml marinelli beaker for 720 hours to allow for radon and its short lived progenies to reach secular equilibrium prior to gamma ray measurement.

For water samples, 500ml of each sample was transferred into the marinelli beaker; then sealed and kept for at least 720 hours, during which time the daughter of radon achieves equilibrium with its short lived progenies and then the sample was ready for analysis by the gamma spectroscopy.

3.6 Measurement of Activity concentration of the Radionuclide

The activity concentration of the prepared soil and water samples was measured using a GMD20 model gamma ray spectrometer shown in Figure 3.1. A GDM20 model consists of a Sodium Iodide Thallium NaI(Tl) detector crystal optically coupled to a photomultiplier tube (PMT) and its resolution is less than 13%, full width at half maximum(FWHM). The assembly has a pre-amplifier incorporated in it (Mustafa et al., 2012). The detector is enclosed in a 100mm thick lead shield line with cadmium and copper sheets, this arrangement are aimed at minimizing the effect of background and scattered radiation. The detector is connected to a computer with a multi-channel analyser (MCA) with Autodas software installed for data acquisition.

The exact mass of each sample in a marinelli beaker was weighed using a digital beam balance and the marinelli beaker was used to feed the sample into a GDM20 spectrometer.

Spectra collection: To determine the energy of the detected gamma radiation, the spectrum was first energy calibrated. The energy calibration of the GDM20 shown in Figure 3.1, was done using ^{152}Eu , source which was available as a standard source. This sample was allowed to run in the detector for 6000 seconds, and a spectrum obtained with several photo peaks but the spectrum energies ranging from 0.344Mev to 1.41Mev were chosen, which gives the range of a gamma ray photon. (Mattetnik, 1995). After calibration of the detector, the background distribution in the environment around the detector was determined by running the system for the same period of time when an empty marineli beaker was used, its spectrum obtained and stored in the computer using the AutoDas commands.

The spectra were again collected from both the soil and water samples using a sodium iodide gamma ray detector in conjunction with a multi-channel gamma spectrometer with the window set to include the appropriate gamma energy window. The soil and water samples separately were placed in the detector on the thallium doped Sodium iodide crystal in order to analyze the radionuclides present.

The soil and water samples were each run for an average of 6000 seconds and the spectra were collected and stored in the computer using the AutoDas commands. This process was repeated for each soil and water sample to obtain the spectra from the samples collected from Kaserem limestone quarry. Each sample gamma ray spectrum was obtained by subtracting the background radiation from the new spectrum obtained when the detector is operated for 6000 second with a sample inside it. Each gamma ray spectrum obtained was analyzed by Autodas software where photo peaks were fitted and other parameter of the spectrum were obtained and the information needed to calculate the specific activities of the radionuclides present in each sample. The activity of each sample was computed using the equation (Girigisu et al., 2013)

$$S.A = \frac{N}{t m C} \quad (3.1)$$

The associated error was calculated using the equation

$$Error = \frac{\sqrt{N}}{tmC} \quad (3.2)$$

Where **S.A** is the activity concentration of the radionuclide in the sample given in Bq kg^{-1} , **N** is the net count for gamma rays emitted by the source. **C** is the correction coefficient of the

detector system shown in Table 3.1 below, m , is the mass of the sample and, t , is the lifetime of the sample.

The standard error which is a measure of how the mean is varied is calculated using equation 3.3

$$S.E = \frac{SD}{\sqrt{n}} \quad (3.3)$$

3.7 Energy calibration, resolution and efficiency of the detector.

Energy calibration is one of the essential requirements in the nuclear spectroscopy. In order to identify the photo peaks with the spectra, the pulse height scale has to be calibrated in terms of gamma ray energy.

In the study, the energy calibration of the GDM-20 NaI (TI) detector shown in Figure 3.1 below was done using ^{152}Eu source which was available standard source supplied by IAEA. This source was placed in the detector and it run for 6000 seconds, a spectrum was obtained having several photo peaks but peaks of energy ranging from 0.344MeV to 1.41MeV were chosen which is the range of gamma ray photon (Mattetnik, 1995). This was chosen because all radionuclides of interest have energies in this range. Channel positions corresponding to 0.344MeV and 1.41MeV peak were determined using the autodos commands "cen" and "cal" which could designate energy in MeV to a particular peak position. With the two commands, the spectrum was energy calibrated and the channel scale was replaced with a new energy scale (Mattetnik, 1995).

The basis for nuclear spectroscopy is location of spectral lines arising from the total absorption of charged particles or photons. For this purpose, the resolution of the detector is important if spectral lines that are so close together are to be separated and observed. Resolution is defined as the ratio full width at half maximum (FWHM) of the full energy peak (photo peak) to the energy midpoint of full energy peak.

$$\text{Resolution} = \frac{\text{FWHM}}{E} \quad (3.3)$$

Where, E is the midpoint of full energy peak. The smaller the energy spread, FWHM, the better is the ability of detector to separate full energy peaks that are close together (Cember, 2009). The energy resolution of scintillation detectors, NaI(Tl) in particular is normally between 7-9% for gamma radiation of energy of about 1MeV.

Efficiency of the detector is a measure of the percentage of radiation that a given detector detects from the overall yield that is estimated from the source.

Detector efficiency (ϵ_t) is the ratio of the total number of counts per unit time over the whole spectrum to the number of gamma rays emitted by the source per unit time. It is given by the equation (Hossain et al., 2012).

$$\epsilon_t = \frac{c_t}{N_\gamma} \times 100\% \quad (3.4)$$

where, c_t , is the total number of counts per unit time over the whole recorded spectrum minus the background.

N_γ is the number of gamma rays emitted by the source per unit time, NaI(Tl) is more efficient in detecting radionuclides than High Purity Germanium (HPGe) detector because of high density of the crystal and high effective atomic number (Cember, 2009). High Purity Germanium (HPGe) detector detects only those radionuclides with low energy efficiency than nuclides with higher energy (Hossain et al., 2012).

The correction coefficients C of the system are presented in the Table 3.1

Table 3.1: Correction coefficients of radionuclides

Energy (KeV)	Decay Series	Coefficient (C)
84.00	Th (Th-228)	0.0286
185.00	U (Ra-226)	0.0043
205-238	Th (Pb-212)	0.0608
242.00	U (Pb-214)	0.0404
295.00	U (Pb-214)	0.0237
309-352	U (Pb-214)	0.0300
538-580	Th (TI-208)	0.0101
610.00	U (Bi-214)	0.0210
780.00	Eu- 152	0.0296
860.56	Th (TI-208)	0.00001254
1170.00	Co-60	0.0200
1460.00	K-40	0.00234

CHAPTER FOUR: RESULTS OF THE STUDY

4.1 Introduction

This chapter presents how primary data is acquired from the detector, results obtained from the study which includes: specific activities, dose rates and radiological hazard indices for both soil and water samples in the following sections.

4.2 Acquisition of Primary Data

The exact masses of the samples in the marinelli beaker were obtained using a beam balance and were then run in the GDM-20 spectrometer to obtain a spectrum. Figure 3.1 above shows an assembly of a GDM20 spectrometer; while using a GDM20 spectrometer for analysis, the gamma ray spectrum for the radionuclides present in each of the soil and water samples collected from Kaserem limestone quarry area was obtained. The soil and water samples were labeled according to the name of the quarry and position from the centre of the quarry moving radially outwards and following the campus direction as shown in Figure 3.0. For example CKLA was the code name for soil samples from position A (the centre of the quarry); the first letter C- represents the surname of the researcher, followed by KL-representing Kaserem limestone and A- represents the position from where the soil was picked (for the central part of the quarry). For all the soil samples the same criteria was used.

For water samples, the first three letters were maintained while the last letters were changed to represent the source of the water sample. For example CKLS was for the sample collected from the stream and CKLP was for the sample collected from the protected spring

For soil samples from the centre of the quarry, position A (CKLA); the spectrum is shown in Figure 4.0.

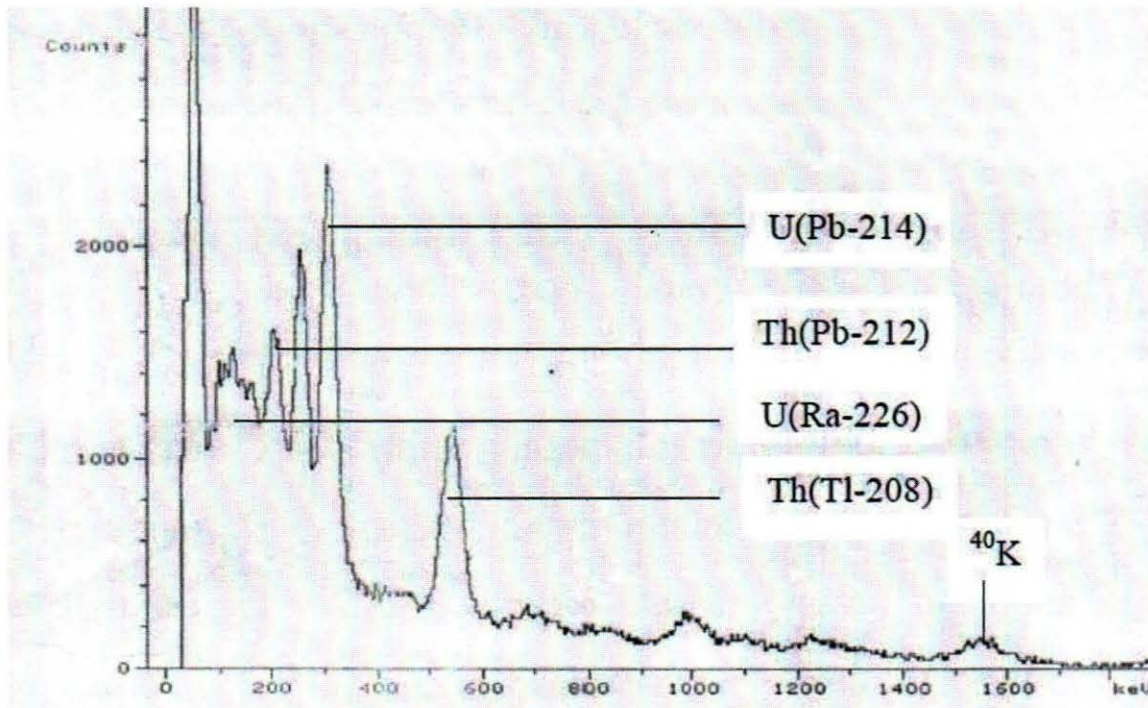


Figure 4.0: Sample spectrum for the soil sample from the central part of the quarry

The sample spectrum used to compute the specific activities of the gamma ray data is shown in Figure 4.0 above. This spectrum was obtained by stripping off the background spectrum using the autodas commands. From the spectrum, five prominent peaks were identified and Autodas software analysis of the spectrum gave the information needed to compute the specific activities of the radionuclides present in the sample. These information read from the spectrum includes: the Centroid energy, standard deviation (S.D), Full Width at Half Maximum (FWHM), sum (N) and the Rate (R). The radionuclides in the chosen photo peaks were identified using the Centroid energy of the peaks. The actual mass of each sample was measured using a digital balance before running the sample in the GDM20 spectrometer to obtain this spectrum

Using the correction coefficients shown in Table 3.1, and applying equations 3.1 and 3.2, the specific activities and the uncertainties of the radionuclides present were computed. The information from the spectrum in the Figure 4.0 and the respective radionuclides are shown in Table 4.0.

Sample ID: CKLA, Sample mass = 0.8048kg, live time = 6019s

Table 4.0: Radionuclides corresponding to each peak for the soil sample from location A

Radionuclide	Photo peak	Centroid (keV)	S.D (keV)	FWHM (keV)	Sum (N)	Rate (s^{-1})	S.A ($Bqkg^{-1}$)
U(Ra-226)	1	108.284	11.371	26.722	1987	0.33	95.39
Th(Pb-212)	2	198.201	10.808	25.399	7758	1.29	23.55
U(Pb-214)	3	304.249	24.182	56.827	2594	0.43	22.59
Th(Tl-208)	4	528.586	36.709	86.267	3669	0.61	74.99
K-40	5	1268.150	29.064	68.301	7850	1.30	692.53

The table 4.0 shows the photo peak values for soil samples corresponding to location A. The radionuclides corresponding to each peak for B (a 50m radius from A), C (a 100m radius from A), D (a 150m radius from A) and E (a 600m radius from A) are shown in Appendix A.

Specific Activity of the soil sample: Using the information given in Table 3.1 and Table 4.0 and applying Equations (3.1) and (3.2) stated previously to each soil sample from each sampled location, the specific activities and their associated errors for the radionuclides present in soil from the central location of the quarry (A) were calculated and presented in the Table 4.1. Analysis of data was done using Microsoft excel package and MATLAB software.

Table 4.1: Specific activities of soil samples from the central part of the quarry

ID	SPECIFIC ACTIVITY (Bqkg ⁻¹)			
	²²⁶ Ra	²³² Th	²³⁸ U	⁴⁰ K
CKLA1	95.39 ± 2.14	49.27 ± 0.75	22.59 ± 0.44	692.53 ± 7.82
CKLA2	35.43 ± 1.15	67.41 ± 0.78	37.09 ± 0.50	916.24 ± 7.90
CKLA3	28.15 ± 1.07	61.58 ± 0.77	17.06 ± 0.36	762.11 ± 7.58
CKLA4	50.35 ± 1.51	75.87 ± 0.92	11.12 ± 0.30	889.46 ± 8.62
CKLA5	42.25 ± 1.25	74.96 ± 0.82	46.43 ± 0.56	850.28 ± 7.60
CKLA6	53.08 ± 1.45	72.86 ± 0.84	17.15 ± 0.35	660.60 ± 6.93
CKLA7	65.17 ± 1.57	69.89 ± 0.81	42.05 ± 0.54	634.70 ± 6.66
CKLA8	45.30 ± 1.34	80.07 ± 0.88	18.32 ± 0.36	853.07 ± 7.89
CKLA9	23.92 ± 0.95	40.15 ± 0.60	59.50 ± 0.64	781.69 ± 7.38
CKLA10	51.71 ± 1.39	39.87 ± 0.60	22.50 ± 0.39	883.58 ± 7.81

From Table 4.1 shows the specific activities of ²²⁶Ra which ranged from 23.92±0.95 Bqkg⁻¹ to 95.39±2.14 Bqkg⁻¹ with a mean of 49.08±1.38 Bqkg⁻¹, while that of ²³²Th ranged from 39.87±0.60 Bqkg⁻¹ to 80.07±0.88 Bqkg⁻¹ with a mean of 63.19±0.78 Bqkg⁻¹ that of ²³⁸U ranged from 11.12±0.30 Bqkg⁻¹ to 59.50±0.64 Bqkg⁻¹ with a mean of 29.38±0.44 Bqkg⁻¹ and that of ⁴⁰K ranged from 634.70±6.66 Bqkg⁻¹ to 916.24±7.90 Bqkg⁻¹ with a mean of 792.43±7.62 Bqkg⁻¹.

The tables showing the specific activities for all the other sampled locations B, C, D and E are shown in appendix B. The same formulas were applied to the spectrums obtained for water samples and results are put in table form as shown in appendix B.

4.2 Specific Activities of Radionuclides

The specific activities of the naturally occurring radionuclides present in both soil and water samples were determined using equations 3.1 and 3.2, at the same time applying correction coefficients shown in Table 3.1. The mean specific activities of radionuclides present in the following samples are presented in the tables in the following sub sections:

4.2.1 Soil samples

The mean specific activities of the radionuclides from the soil samples for each sampled location around Kaserem limestone quarry area is computed and tabulated as shown in Table 4.2.

Table 4.2: Mean activities for radionuclides in soil samples from each location around the quarry

SAMPLE ID	SPECIFIC ACTIVITY (Bqkg ⁻¹)			
	²²⁶ Ra	²³² Th	²³⁸ U	⁴⁰ K
CKLA(centre)	49.08 ± 1.38	64.69 ± 0.79	29.38 ± 0.44	792.43 ± 7.62
CKLB(50m)	95.09 ± 2.49	99.90 ± 1.26	51.78 ± 0.77	672.92 ± 8.96
CKLC(100m)	80.19 ± 2.28	71.48 ± 1.06	40.59 ± 0.69	470.67 ± 7.41
CKLD(150m)	79.12 ± 2.20	89.73 ± 1.41	47.52 ± 0.73	286.93 ± 5.47
CKLE(600m)	75.06 ± 2.35	59.23 ± 1.04	36.06 ± 0.69	461.75 ± 7.90

The Table 4.2 shows the mean activities of ²²⁶Ra, ²³²Th, ²³⁸U and ⁴⁰K for all the sampled locations around the quarry and they ranged from 49.08±1.38 Bqkg⁻¹ to 95.09±2.49 Bqkg⁻¹, 59.23±1.04 Bqkg⁻¹ to 99.90±1.26 Bqkg⁻¹, 36.06±0.69 Bqkg⁻¹ to 51.78±0.77 Bqkg⁻¹ and 286.93±5.47 Bqkg⁻¹ to 792.43±7.62 Bqkg⁻¹ respectively.

A graph of mean activity of the radionuclides for all the selected locations of the soil samples in and around the quarry is presented in the Figure 4.3 below. The graph shows that the central location A and B have very high concentration of all other locations in ⁴⁰K. However in all the sampled locations ⁴⁰K, is abundant.

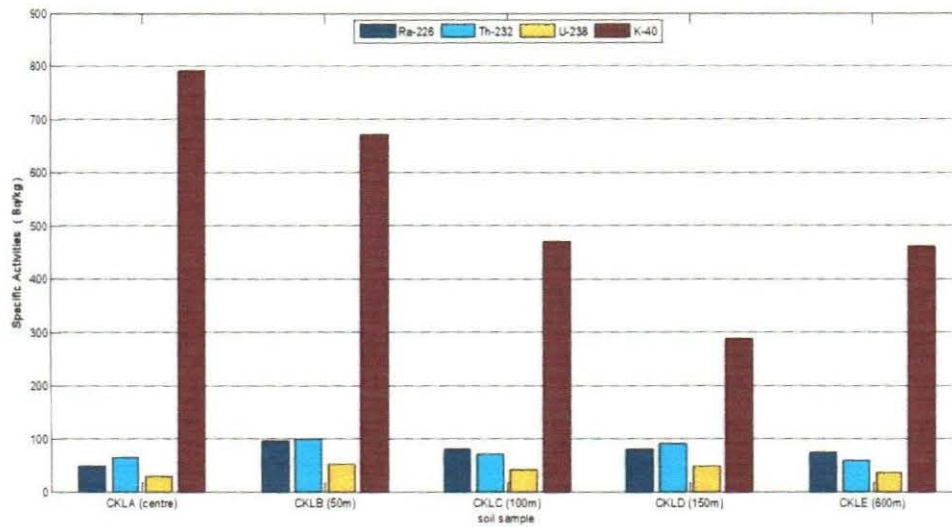


Figure 4.1: A bar graph showing mean activities for the soil sampled from all locations around the quarry

The overall mean standard deviation and standard error for all the soil sampled locations were computed and presented in Table 4.3

Table 4.3: Overall mean and standard deviation of activities for all soil samples from the selected locations around the quarry

Radionuclides	²²⁶ Ra	²³² Th	²³⁸ U	⁴⁰ K
Overall Mean(Bqkg ⁻¹)	75.71	77.01	41.07	536.94
Standard Deviation(SD)	25.84	21.06	17.30	230.64
Standard Error(SE)	3.65	2.98	2.45	32.62

Table 4.3 shows, the overall mean of all the identified radionuclides present in the quarry. Which were computed from equations 3.1, 3.2 and 3.3, the specific activities, uncertainties and standard error for all the samples. This was done by finding the average specific activity and error for all the fifty samples using Microsoft excel package; this was done to minimize error created during computations. The computation for standard error was done taking into consideration the standard deviation using equation 3.3

The overall mean specific activities of ^{226}Ra , ^{232}Th , ^{238}U and ^{40}K for all soil samples were: $76\pm 4 \text{ Bqkg}^{-1}$, $77\pm 3 \text{ Bqkg}^{-1}$, $41\pm 2 \text{ Bqkg}^{-1}$ and $537\pm 33 \text{ Bqkg}^{-1}$ respectively. These values have been written with their standard errors which were computed from the standard deviation.

4.2.2: Water samples

The specific activities for the two water sources were calculated, using the same identification Table 4.0, radionuclides present in water samples were identified and their specific activities were computed and presented as shown in Table 4.4.

Table 4.4: Overall mean specific activities of radionuclide of water samples.

ID	SPECIFIC ACTIVITY (Bqkg^{-1})			
	^{226}Ra	^{232}Th	^{238}U	^{40}K
CKLS	92.65 \pm 2.53	8.83 \pm 0.38	14.36 \pm 0.44	12.45 \pm 1.14
CKLP	115.70 \pm 2.81	24.33 \pm 0.65	24.17 \pm 0.56	33.00 \pm 1.97
MEAN	104.18 \pm 2.67	16.58 \pm 0.52	19.27 \pm 0.50	22.73 \pm 1.56
STDEV	44.77 \pm 0.64	5.57 \pm 0.09	3.20 \pm 0.05	17.55 \pm 0.66

From the Table 4.4, the overall mean of the specific activities of the radionuclides present in the water samples with sample ID-CKLS representing water samples from the nearby stream while CKLP represents water samples from the protected spring (Protected spring here means piped water from underground).

The mean specific activities of ^{226}Ra , ^{232}Th , ^{238}U and ^{40}K for all the water sources sampled around the quarry area ranged from $92.65\pm 2.53 \text{ Bq kg}^{-1}$ to $115.70\pm 2.81 \text{ Bq kg}^{-1}$, $8.83\pm 0.38 \text{ Bq kg}^{-1}$ to $24.33\pm 0.65 \text{ Bq kg}^{-1}$, $14.36\pm 0.44 \text{ Bq kg}^{-1}$ to $24.17\pm 0.56 \text{ Bq kg}^{-1}$ and $12.45\pm 1.14 \text{ Bq kg}^{-1}$ to $33.00\pm 1.97 \text{ Bq kg}^{-1}$ respectively. Their overall mean specific activities for all the water sources sampled are represented in a bar graph shown in Figure 4.2.

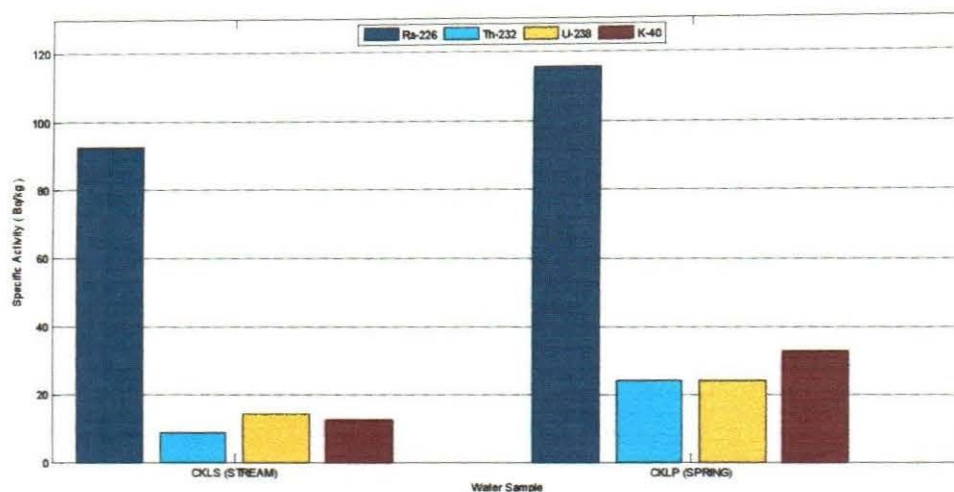


Figure 4.2: A bar graph showing mean specific activities of radionuclides for the water samples collected

The graph shows that ^{226}Ra concentration is higher in the water samples analyzed than all the other radionuclides. This is attributed to weathered particles of igneous rocks on the land associated with naturally occurring radionuclides having been deposited on the stream and spring.

Table 4.5: Overall average specific activity concentration with their standard error of both soil and water from Kaserem limestone quarry area

Radionuclides	^{226}Ra	^{232}Th	^{238}U	^{40}K
Soil samples(Bqkg ⁻¹)	75.71±3.65	77.01±2.98	41.07±2.45	536.94±32.62
Water sample(Bqkg ⁻¹)	104.93 ±13.93	16.58 ±3.09	19.27±1.91	22.73±6.39

Soil Samples from this quarry were found to have high specific activities of Thorium and Uranium. This might be as a result of the geological outline of the area showing that the soil might have been formed from carbonate and monazite rocks which are rich in these radionuclides.

4.3. Dose rate values

The Absorbed dose rate in indoor air (D) in nGy hr^{-1} and the corresponding annual effective dose (AED) in mSv y^{-1} due to gamma ray emissions from naturally occurring radionuclides present in soil and water samples were calculated using the formulae stated in equations (2.23) and (2.24) respectively.

Table 4.6: Absorbed dose rates (D) for both soil and water samples.

Soil	CKLA	CKLB	CKLC	CKLD	CKLE
D (nGy hr^{-1})	97.85 ± 1.44	135.68 ± 2.29	101.80 ± 1.99	105.53 ± 2.11	91.11 ± 2.03
Water	CKLS	CKLP			
D (nGy hr^{-1})	45.94 ± 1.38	66.93 ± 1.72			

Table 4.6 presents the total absorbed dose rate values (D) of 1m above in air arising from both soil and water samples. For soil samples the values varied from $91.11 \pm 2.03 \text{ nGy hr}^{-1}$ to $135.68 \pm 2.29 \text{ nGy hr}^{-1}$ while for water samples it ranged from $45.94 \pm 1.38 \text{ nGy hr}^{-1}$ to $66.93 \pm 1.72 \text{ nGy hr}^{-1}$.

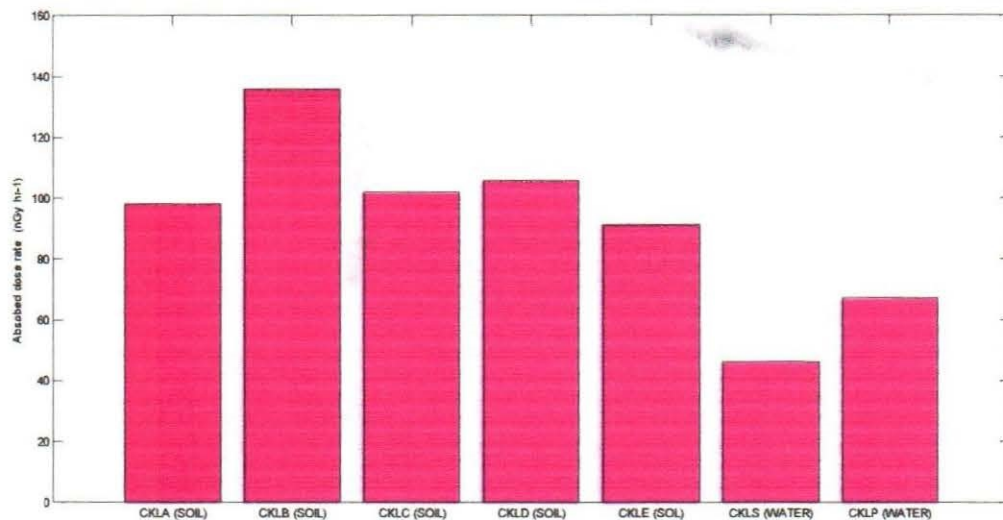


Figure 4.3: A graph showing absorbed dose rates in both soil and water

Figure 4.3 shows that all the absorbed dose rates calculated are below, 140nGy hr^{-1} for both soil and water samples.

Table 4.6: Annual effective dose rates, (AED) for both soil and water samples.

Soil	CKLA	CKLB	CKLC	CKLD	CKLE
AED (mSv y^{-1})	0.273 ± 0.004	0.391 ± 0.007	0.295 ± 0.006	0.309 ± 0.006	0.263 ± 0.006
Water	CKLS	CKLP			
AED (mSv y^{-1})	0.143 ± 0.004	0.207 ± 0.005			

Table 4.6 above, shows the calculated values of annual effective dose rate for all the soil samples collected ranged from $0.273\pm 0.004 \text{ mSv y}^{-1}$ to $0.391\pm 0.007 \text{ mSv y}^{-1}$. While for water samples it ranged from $0.143\pm 0.004 \text{ mSv y}^{-1}$ to $0.207\pm 0.005 \text{ mSv y}^{-1}$ which are more than the world average value of 0.07 mSv y^{-1} .

4.4 Radiation hazard indices

Radium equivalent values: Radium equivalent was calculated using equation (2.25) and the results for both soil and water samples were presented in Table 4.7

Table 4.7: Radium equivalent values for both soil and water samples.

Soil	CKLA	CKLB	CKLC	CKLD	CKLE
Ra_{eq} (Bqkg^{-1})	202.60 ± 3.10	289.77 ± 4.99	218.64 ± 4.37	229.53 ± 4.63	195.31 ± 4.44
Water	CKLS	CKLP			
Ra_{eq} (Bqkg^{-1})	106.24 ± 3.16	153.04 ± 3.89			

From the Table 4.7 above, the radium equivalent activity owing to the activity concentration of the radionuclides from all the sites varied from $106.24\pm 3.16 \text{ Bqkg}^{-1}$ to $289.77\pm 4.99 \text{ Bqkg}^{-1}$ for both soil and water samples which values are much less than the threshold value of 370 Bqkg^{-1}

The graph to show how hazardous the soil and water sample from the selected locations and sources of water was plotted and is shown in Figure 4.4

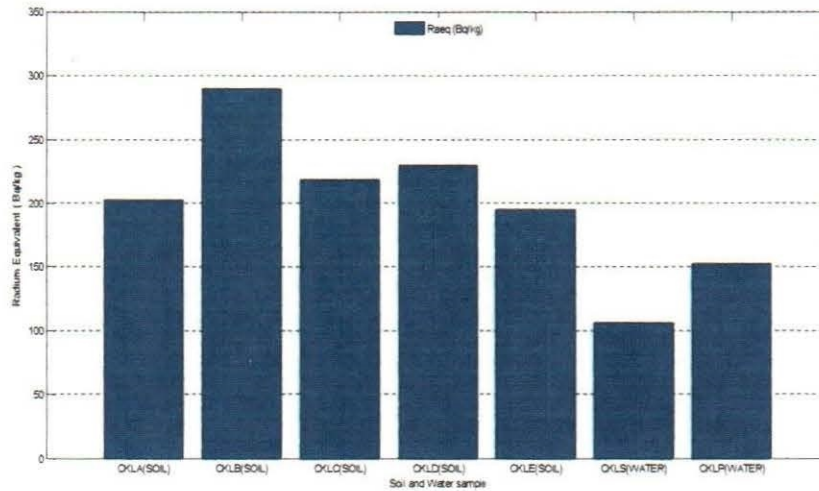


Figure 4.4: A graph showing Radium equivalent for both soil and water samples

The Figure 4.4 shows that, the radium equivalent for soil samples is higher for all soil samples from a location 50m (CKLB) from the centre of the quarry while for water it was higher for water samples from the protected spring (CKLP). The soil at 50 m from the centre of the quarry had just been excavated and having milled stones which could be having a high concentration of mineral ore than all the other sites sampled, while water from the protected spring is piped water from underground where stones lie. Corroded pipes and high mineral concentration underground is associated with high naturally occurring radionuclides (NORM) Radiological hazard indices for both soil and water from Kaserem limestone quarry was computed based on the formulae for hazard indices, given in equations (2.26) for internal hazard index while for external hazard index, equation (2.27). The internal and external hazard indices are given in tables 4.8 and 4.9 respectively.

Table 4.8: Internal hazard indices, (H_{in}) for both soil and water samples.

Soil	CKLA	CKLB	CKLC	CKLD	CKLE
H_{in} ($mSv\ y^{-1}$)	0.68 ± 0.01	1.04 ± 0.02	0.81 ± 0.02	0.83 ± 0.02	0.73 ± 0.02
Water	CKLS	CKLP			
H_{in} ($mSv\ y^{-1}$)	0.54 ± 0.02	0.73 ± 0.02			

Table 4.8 shows that the values of internal hazard index for both soil samples ranged from $0.68 \pm 0.01 \text{ mSv y}^{-1}$ to $1.04 \pm 0.02 \text{ mSv y}^{-1}$ and for water samples it ranged from $0.54 \pm 0.02 \text{ mSv y}^{-1}$ to $0.73 \pm 0.02 \text{ mSv y}^{-1}$. All these values were less than the world average value of 1 mSv y^{-1} .

Table 4.9: External hazard indices, (H_{ex}) for both soil and water samples.

Soil	CKLA	CKLB	CKLC	CKLD	CKLE
H_{ex} (mSv y^{-1})	0.55 ± 0.01	0.78 ± 0.01	0.62 ± 0.01	0.53 ± 0.01	0.26 ± 0.01
Water	CKLS	CKLP			
H_{ex} (mSv y^{-1})	0.29 ± 0.01	0.41 ± 0.01			

From Table 4.9, the external hazard index value for all the soil sampled locations is ranged from $0.26 \pm 0.01 \text{ mSv y}^{-1}$ to $0.78 \pm 0.01 \text{ mSv y}^{-1}$, while that of the water samples ranged from $0.29 \pm 0.01 \text{ mSv y}^{-1}$ to $0.41 \pm 0.01 \text{ mSv y}^{-1}$ which values are all less than 1 mSv y^{-1} .

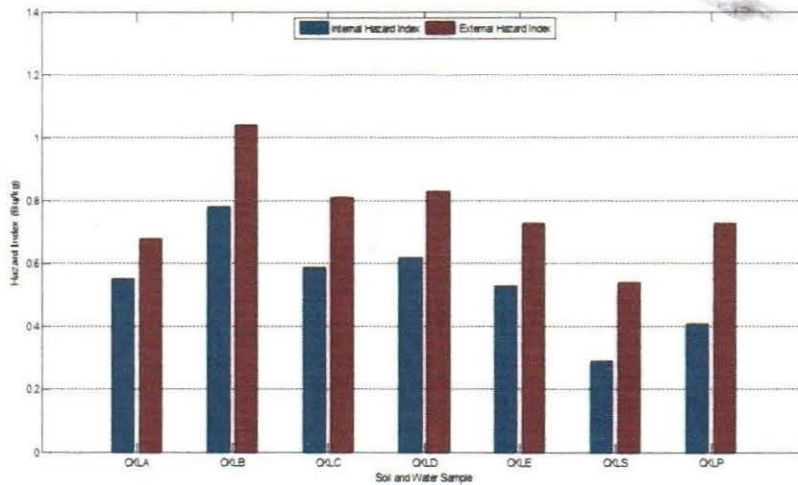


Figure 4.5: A graph showing Hazard indices in soil and water samples

The graph above shows that, all the internal hazard indices calculated are less than unity however the external hazard index at the second location is greater than unity and overall mean of the external hazard index exceeds the internal hazard index in all locations for both soil and water samples.

Comparison of activity concentration of soil samples from Kaserem quarry area with similar studies worldwide. The activity concentrations of ^{226}Ra , ^{232}Th , ^{238}U and ^{40}K in soil from this study were compared with similar studies from other countries and are presented in table 4.10

Table 4.10: Comparison of activity concentrations with similar studies

Country	^{226}Ra (Bqkg ⁻¹)	^{232}Th (Bqkg ⁻¹)	^{238}U (Bqkg ⁻¹)	^{40}K (Bqkg ⁻¹)	Reference
Saudi Arabia	14.5 ± 3.9	11.2 ± 3.9	-	255 ± 63	Alaamer, 2007
Pakistan	21.7 ± 4.4	31 ± 6.6	-	392 ± 83	Fatima et al., 2008
Egypt	20.40	4.40	-	19.30	Sharaf et al., 1999
Ghana	13.61	24.22	-	162.08	Faanu et al., 2011
Nigeria	-	26.4	55.3	505.1	Ademola, 2014
Kenya	28.7 ± 3.6	73.3 ± 9.1	-	255.7 ± 38.5	Mustapha et al., 1999
Kenya	93.40	150.50	-	732.60	Kinyua et al., 2011
Kenya	20.90	27.60	-	69.50	Osoro et al., 2011
Tanzania	-	36.4	51.7	564.3	Najat et al 2013
World average	35.00	30.00	35.00	400.00	UNSCEAR, 2000
Egypt	-	18.00	37.00	320.00	UNSCEAR, 2000
China	-	41.00	32.00	440.00	UNSCEAR, 2000
Hong Kong	-	95.00	84.00	530.00	UNSCEAR, 2000
Uganda	-	768.40	56.00	1702.10	Mugaiga et al., 2016
Uganda	-	216.53	55.33	566.93	Turyahabwa et al., 2016
Kaserem Limestone Quarry(Uganda)	75.71	77.01	41.01	536.94	Present study

The Table 4.10 shows results on similar studies carried out in Uganda and other countries. The measured activity concentrations of radionuclides ^{226}Ra , ^{232}Th , ^{238}U and ^{40}K were compared with values reported both within Uganda and other countries. It is found that the measured activity concentrations of the four (4) radionuclides in this study are higher than

most of the reported values from other countries as well as the world average values. However these values are lower than the values reported by Mugaiga et al.(2016) and Turyahabwa et al.,(2016) for the three (3) radionuclides ^{232}Th , ^{238}U and ^{40}K in soil and rock samples measured.

CHAPTER FIVE: DISCUSSIONS, CONCLUSIONS AND RECOMMENDATIONS

5.1. Discussion of results

This chapter describes the discussions of the results obtained, conclusions and recommendations. The discussion of results was based on the objectives of the study. The specific activities of radionuclides and radiological indices in soil and water from Kaserem limestone quarry area are discussed in this section.

Specific activities

The specific activities and mean activities of each soil sampled location around the quarry were calculated and the results of all these soil and water samples are presented in detail in appendix A. From Table 4.1.B in the appendix B, the central sample location A, had the specific activities of ^{226}Ra ranged from $23.92 \pm 0.95 \text{ Bqkg}^{-1}$ to $95.39 \pm 2.14 \text{ Bqkg}^{-1}$ with a mean of $49.08 \pm 1.38 \text{ Bqkg}^{-1}$, while that of ^{232}Th ranged from $39.87 \pm 0.60 \text{ Bqkg}^{-1}$ to $80.07 \pm 0.88 \text{ Bqkg}^{-1}$ with a mean of $63.19 \pm 0.78 \text{ Bqkg}^{-1}$, that of ^{238}U ranged from $11.12 \pm 0.30 \text{ Bqkg}^{-1}$ to $59.50 \pm 0.64 \text{ Bqkg}^{-1}$ with a mean of $29.38 \pm 0.44 \text{ Bqkg}^{-1}$ and that of ^{40}K ranged from $634.70 \pm 6.66 \text{ Bqkg}^{-1}$ to $916.24 \pm 7.90 \text{ Bqkg}^{-1}$ with a mean of $792.43 \pm 7.62 \text{ Bqkg}^{-1}$. These values were generally higher than the world average values published by UNSCEAR, (2000) which are 35 Bqkg^{-1} , 30 Bqkg^{-1} , 35 Bqkg^{-1} and 400 Bqkg^{-1} respectively for ^{226}Ra , ^{232}Th , ^{238}U and ^{40}K . The results of study compare well with the result obtained for soil samples in Hong Kong as stated in UNSCEAR, (2000) shown in (Table 4.10). This means that the radiations from the soil is high hence the soil may be dangerous to the health of the people if used for construction.

In the sample location B, a radius of 50 m from location A, as shown in Table 4.2.B, the specific activities of ^{226}Ra ranged from $69.02 \pm 2.14 \text{ Bqkg}^{-1}$ to $122.28 \pm 2.92 \text{ Bqkg}^{-1}$ with a mean of $95.09 \pm 2.49 \text{ Bqkg}^{-1}$, that of ^{232}Th is $87.55 \pm 1.10 \text{ Bqkg}^{-1}$ to $125.14 \pm 1.48 \text{ Bqkg}^{-1}$ with a mean of $97.54 \pm 1.24 \text{ Bqkg}^{-1}$, while that of ^{238}U ranged from $29.64 \pm 0.58 \text{ Bqkg}^{-1}$ to $92.10 \pm 1.10 \text{ Bqkg}^{-1}$ with a mean of $51.78 \pm 0.77 \text{ Bqkg}^{-1}$ and that of ^{40}K ranged from $388.80 \pm 0.88 \text{ Bqkg}^{-1}$ to $837.34 \pm 10.54 \text{ Bqkg}^{-1}$ with a mean of $672.92 \pm 8.96 \text{ Bqkg}^{-1}$. The distribution of the radionuclides is not uniform in all the sampled locations and the activities of radionuclides in this portion is much higher than all the other sampled locations, this is because the soils

collected from this site contained milled stones which could be having a higher concentration of mineral ores which are associated with a higher background radiation. In all locations ^{40}K is the most abundant and ^{238}U had the least concentration. According to world averages of activity concentrations of ^{226}Ra , ^{232}Th , ^{238}U and ^{40}K the mean activity of ^{226}Ra is almost three times the world average of 35 Bqkg^{-1} while that of ^{232}Th is more than three times the world average value of 30 Bqkg^{-1} and that of ^{40}K is more than the world average value of 400 Bqkg^{-1} (UNSCEAR, 2000). In comparison with other similar studies in other countries (Table 4.10), it's observed that, the mean Values in this quarry is lower than those obtained by Kinyua et al., (2011) , Mugaiga et al.,(2016) and Turyahabwa et al.,(2016) for the three (3) radionuclides ^{232}Th , ^{238}U and ^{40}K in soil and rock samples measured.

In the sample location C, a radius of 100 m from A, as shown in Table 4.3.B, in the appendix B, the specific activities of ^{226}Ra ranged from $38.41 \pm 1.43 \text{ Bqkg}^{-1}$ to $115.66 \pm 2.85 \text{ Bqkg}^{-1}$ with a mean of $80.19 \pm 2.28 \text{ Bqkg}^{-1}$, while that of ^{232}Th ranged from $52.08 \pm 0.93 \text{ Bqkg}^{-1}$ to $94.77 \pm 1.22 \text{ Bqkg}^{-1}$ with a mean of $69.24 \pm 1.04 \text{ Bqkg}^{-1}$, that of ^{238}U ranged from $21.97 \pm 0.50 \text{ Bqkg}^{-1}$ to $61.83 \pm 0.87 \text{ Bqkg}^{-1}$ with a mean of $40.59 \pm 0.69 \text{ Bqkg}^{-1}$ and that of ^{40}K ranged from $190.97 \pm 5.19 \text{ Bqkg}^{-1}$ to $832.81 \pm 10.55 \text{ Bqkg}^{-1}$ with a mean of $470.67 \pm 7.41 \text{ Bqkg}^{-1}$. These values were generally higher than the world average values published by UNSCEAR, (2000) which are 35 Bqkg^{-1} , 30 Bqkg^{-1} , 35 Bqkg^{-1} , and 400 Bqkg^{-1} respectively for ^{226}Ra , ^{232}Th , ^{238}U and ^{40}K . All the values were lower than that obtained by Kinyua et al., (2011) in Tabaka soapstone quarry in Kenya.

In the sample location D, as shown in Table 4.4 B, in the appendix B, which is a radius of 150 m from the centre A, the specific activities of ^{226}Ra ranged from $18.36 \pm 1.09 \text{ Bqkg}^{-1}$ to $101.46 \pm 2.38 \text{ Bqkg}^{-1}$ with a mean of $79.12 \pm 2.22 \text{ Bqkg}^{-1}$, while that of ^{232}Th ranged from $59.45 \pm 1.00 \text{ Bqkg}^{-1}$ to $123.91 \pm 1.40 \text{ Bqkg}^{-1}$ with a mean of $83.79 \pm 1.13 \text{ Bqkg}^{-1}$, that of ^{238}U ranged from $26.19 \pm 0.57 \text{ Bqkg}^{-1}$ to $75.90 \pm 0.96 \text{ Bqkg}^{-1}$ with a mean of $47.52 \pm 0.73 \text{ Bqkg}^{-1}$ and that of ^{40}K ranged from $32.40 \pm 1.82 \text{ Bqkg}^{-1}$ to $621.82 \pm 8.90 \text{ Bqkg}^{-1}$ with a mean of $286.93 \pm 5.47 \text{ Bqkg}^{-1}$. The concentration of ^{226}Ra is two times higher than the world average value of 35 Bqkg^{-1} , that of ^{232}Th is also two times higher than 30 Bqkg^{-1} while that of ^{40}K is lower than the world average of 400 Bqkg^{-1} . The value for ^{226}Ra is higher than all those obtained by other researchers as in table 4.09, however that of ^{232}Th and

^{40}K are close to the values obtained by Mustapha, (1999). Lower values were obtained by Faanu et al., (2011) in Ghana, Alaamer, (2007) in Saudi Arabia.

Lastly, in the sample location E, a radius of 600 m from the centre A, whose specific activities are shown in Table 4.5.B in the appendix B, revealed that the specific activities of ^{226}Ra ranged from $56.38 \pm 1.90 \text{ Bqkg}^{-1}$ to $92.78 \pm 2.67 \text{ Bqkg}^{-1}$ with a mean of $75.06 \pm 2.35 \text{ Bqkg}^{-1}$, while that of ^{232}Th ranged from $46.30 \pm 0.91 \text{ Bqkg}^{-1}$ to $65.91 \pm 1.12 \text{ Bqkg}^{-1}$ with a mean of $58.65 \pm 1.03 \text{ Bqkg}^{-1}$, that of ^{238}U ranged from $29.23 \pm 0.61 \text{ Bqkg}^{-1}$ to $42.03 \pm 0.77 \text{ Bqkg}^{-1}$ with a mean of $36.06 \pm 0.69 \text{ Bqkg}^{-1}$ and that of ^{40}K ranged from $320.50 \pm 6.16 \text{ Bqkg}^{-1}$ to $560.69 \pm 8.93 \text{ Bqkg}^{-1}$ with a mean of $461.75 \pm 7.90 \text{ Bqkg}^{-1}$.

From the results above, which are summarized in Table 4.1, the radionuclides present in the soil samples have no particular relationship between the specific activity and the radius of the point of location within and outside the quarry; this is attributed to the fact that there may have been mixing of rock debris and excavated soil. In all the locations ^{40}K had the highest activity concentration. This is due to heterogeneous soil characteristics. The variation of natural radioactivity at different sampling locations was due to the variation of radionuclide in the geological formations. According to Kinyua et al., (2011), younger granites represent the highest elevation of naturally occurring radionuclides while the lower elevation naturally occurring radionuclides is in the older rocks. This may be attributed to the presence of relatively increased amount of accessory minerals such as zircon, iron oxide, fluorite and other radioactive related minerals. These minerals play an important role in controlling the distribution of Uranium and Thorium (Faanu et al., 2011; Mugaiga et al., 2016 & Turyahabwa et al., 2016)

There were two water sources around the quarry and the first was a stream of running water, the specific activities of ^{226}Ra ranged from $24.97 \pm 1.35 \text{ Bqkg}^{-1}$ to $128.28 \pm 3.05 \text{ Bqkg}^{-1}$ with a mean of $92.65 \pm 2.53 \text{ Bqkg}^{-1}$, while that of ^{232}Th ranged from $4.40 \pm 0.26 \text{ Bqkg}^{-1}$ to $15.48 \pm 0.52 \text{ Bqkg}^{-1}$ with a mean of $8.83 \pm 0.38 \text{ Bqkg}^{-1}$, that of ^{238}U ranged from $12.12 \pm 0.40 \text{ Bqkg}^{-1}$ to $18.36 \pm 0.51 \text{ Bqkg}^{-1}$ with a mean of $14.36 \pm 0.44 \text{ Bqkg}^{-1}$ and that of ^{40}K ranged from $2.16 \pm 0.54 \text{ Bqkg}^{-1}$ to $32.29 \pm 2.05 \text{ Bqkg}^{-1}$ with a mean of $12.45 \pm 1.14 \text{ Bqkg}^{-1}$. The value of radium was higher than all the other radionuclides; however all the other radionuclides were below the world average.

The other source was a protected spring, the specific activities of ^{226}Ra ranged from $66.30 \pm 2.20 \text{ Bqkg}^{-1}$ to $176.69 \pm 3.45 \text{ Bqkg}^{-1}$ with a mean of $115.70 \pm 2.81 \text{ Bqkg}^{-1}$ whereas that of ^{232}Th ranged from $16.63 \pm 0.55 \text{ Bqkg}^{-1}$ to $35.14 \pm 0.77 \text{ Bqkg}^{-1}$ with a mean of $24.33 \pm 0.65 \text{ Bqkg}^{-1}$, that of ^{238}U ranged from $19.40 \pm 0.51 \text{ Bqkg}^{-1}$ to $28.26 \pm 0.61 \text{ Bqkg}^{-1}$ with a mean of $24.17 \pm 0.56 \text{ Bqkg}^{-1}$ and that of ^{40}K ranged from $11.89 \pm 1.27 \text{ Bqkg}^{-1}$ to $60.03 \pm 2.73 \text{ Bqkg}^{-1}$ with a mean of $33.00 \pm 1.97 \text{ Bqkg}^{-1}$. The value obtained for ^{226}Ra was three times higher than the world average of 35 Bqkg^{-1} while the others were within the range of the world average. This variation is attributed to variation of concentrations of radionuclides in the geological formations and the economic activities taking place around the quarry, such as farming with use of fertilizers which may increase potassium levels.

Radiological hazard indices

Radium equivalent dose rate, $R_{a_{eq}}$, Absorbed dose rate, D , Annual effective dose, AED, and Hazard indices for all the sampled locations were calculated. Location B, had a higher than all the other locations as seen in Table 4.5, Radium equivalent activity for all the soil sampled locations were computed and the mean values were $202.60 \pm 3.10 \text{ Bqkg}^{-1}$, $289.77 \pm 4.99 \text{ Bqkg}^{-1}$, $218.64 \pm 4.63 \text{ Bqkg}^{-1}$, $229.53 \pm 4.49 \text{ Bqkg}^{-1}$ and $195.31 \pm 4.44 \text{ Bqkg}^{-1}$ for sampled locations A, B, C, D and E respectively and for water samples they were $106.20 \pm 3.16 \text{ Bqkg}^{-1}$ and $153.04 \pm 3.89 \text{ Bqkg}^{-1}$ for the stream and protected spring respectively. The mean Radium equivalent for all the sampled locations was $227.17 \pm 4.31 \text{ Bqkg}^{-1}$ for soil samples and for water samples it was $129.64 \pm 3.53 \text{ Bqkg}^{-1}$ which value were below the world average value of 370 Bqkg^{-1} (ICRP, 2000: UNSCEAR, 2000). This means that the soil and water from this quarry poses no much radiation risk to the people working in the quarry and those from the surrounding that consume the water for now but with increased human activities with time it may pose a radiological hazard to the community.

The calculated absorbed dose rate values for soil samples ranged from 91.11 nGyh^{-1} to 135.68 nGyh^{-1} as shown in table 4.8. The computed average absorbed dose rate values for each location were $97.85 \pm 1.44 \text{ nGyh}^{-1}$, $135.68 \pm 2.29 \text{ nGyh}^{-1}$, $101.80 \pm 1.99 \text{ nGyh}^{-1}$, $105.53 \pm 2.11 \text{ nGyh}^{-1}$ and $91.11 \pm 2.03 \text{ nGyh}^{-1}$ for locations A, B, C, D and E respectively while for water samples the absorbed dose rates are $45.94 \pm 1.38 \text{ nGyh}^{-1}$ and $66.93 \pm 1.72 \text{ nGyh}^{-1}$. The values obtained for soil samples are higher than the world average value which is 60 nGyh^{-1}

The ultimate use of the measured activities in building materials is to estimate the radiation dose expected to be delivered externally if a building is constructed using these materials. To limit the Annual external gamma ray dose to 1 mSvy^{-1} (ICRP, 2000), the annual external dose was calculated using equation (2.24), and for all soil samples collected from all locations the average value was 0.31 mSvy^{-1} while that of water samples was 0.18 mSvy^{-1} . Results of these calculations are presented in Table 4.8. All these values are below unity hence the materials used for building from this location pose no significant health risk to the population.

The External hazard index was calculated using equation (2.27) and for all the soil samples the value was 0.61 while that of the water sample was 0.35. Since these values were less than unity then the soil and water may not pose any significant radiological hazard to the population.

5.2. Conclusion

The activity concentrations of ^{226}Ra , ^{232}Th , ^{238}U and ^{40}K in soil samples were 75.71 Bqkg^{-1} , 77.01 Bqkg^{-1} , 41.07 Bqkg^{-1} and 536.94 Bqkg^{-1} respectively. These natural activity values were more than the accepted world average values; hence this area should be considered high background radiation area (HBRA). In water samples the specific activity concentration of ^{226}Ra , ^{232}Th , ^{238}U and ^{40}K were 104.18 Bqkg^{-1} , 16.58 Bqkg^{-1} , 19.27 Bqkg^{-1} and 22.73 Bqkg^{-1} respectively. The mean radium equivalent values for soil and water samples were 227.17 Bqkg^{-1} and 129.64 Bqkg^{-1} respectively. The average absorbed dose rates were found to be 106.39 nGyh^{-1} for soil samples which value is about 2 times the world average of 60 nGyh^{-1} (UNSCEAR, 2000) and 56.44 nGyh^{-1} for water samples and this value is also higher than the world average of 55 nGyh^{-1} . Assuming a 33% occupancy factor for Uganda (Turyahabwa et al., 2016), the annual average effective doses rates were 0.31 mSvy^{-1} and 0.18 mSvy^{-1} for soil and water samples respectively. The value for soil samples is five times the world average value of 0.07 mSvy^{-1} while the value for water samples is higher than 0.12 mSvy^{-1} the world average value for water. The external and internal hazard indices were 0.61 mSvy^{-1} and 0.81 mSvy^{-1} for soil samples and 0.35 mSvy^{-1} and 0.63 mSvy^{-1} for water samples respectively. These values were all below 1 mSvy^{-1} which is the world average value hence soil and water from these sites pose no significant health risk to the users.

5.3. Recommendations

This study was conducted using the soil and water samples collected from Kaserem limestone quarry area. Based on the results and conclusions drawn from this study, the following are recommended:

Precautionary steps such as wearing a type of protective clothing and masks should be taken into consideration by the miners since the level of dust in then crushing sites is high.

Quarrying activities must be supervised and regulated by appropriate authorities especially the Atomic Energy Council of Uganda.

The policy makers should consider the evaluation of the risks associated to natural radionuclides in foodstuffs and vegetation to obtain more data on radiation levels in the studied area.

To estimate the potential radiological health risks in stones, the dose rate associated to radon gas should be investigated as well and further epidemiology on the cause of cancer in the studied area is recommended

REFERENCES

- Abdulkarim, M.S & Umar,S., (2013). An Investigation of Natural Radioactivity around Gold mining sites in Birnin Gwari,North Western Nigeria. *Research journal of physical Sciences*,1,20.
- Ademola, A.K, Bello,A.K, & Adejumobi, A.C., (2014). Determination of Natural Radioactivity and harzzard in soil samples in and around Gold mining area in Itagunmodi, south Western Nigeria. *Journal of radiation research and applied science*, 7,229.
- Aguko,W.O,Kinyua, R& Onger,R, (2013). Assesment of Radiation Exposure level associated with Gold mining in Sakwa Wagusu, Bondo District, Kenya. *Research journal of applied sciences*.
- Alaamer,A.S, (2008). Assessment of human exposures to Natural Radiation in soil of Riyadh Saud Arabia.*Turkish journal of Engineering and Environmental science*,32, 229.
- Alpen, L.E.(1998). *Radiation Biophysics*, 2nd edition, Academic press, California, USA.
- Ali et al.,(2012). Assessment of radiological hazard of NORM in Margalla Hills limestone, Pakistan. *Journal on environmental research*.
- Anguma,S.(1999).Determination of activity levels of Cesium in Lake Victoria, Lake kyoga and naturally occurring radionuclides in their biota. Unpublished master's thesis, Makerere University
- Atambo V.O (2011). Determination of naturally occurring radioactive elements and Radiation exposure levels in the soapstone quarries of Tabaka region of kisii District, Kenya. Published master's thesis.
- Attix, F.H.(1986).*Introduction to radiological physics and Radiation dosimetry*, John Wiley and sons. USA
- Badhan, K & Mehra,R.(2012).Primordial Radioactivity of ^{238}U , ^{232}Th and ^{40}K .Measurement for soils of Ludhiana District, Punjab,India.*Radiation protection Dosimetry*,152,297–32
- Banzi, F.P, Kifanga,L.D & Bundala,F.M (1999). Natural radioactivity and radiation exposure at Majingu phosphate mine in Tanzania, *Journal of Radiation protection*.20:41-51
- Beretka, J & Mathew, P.O (1985).Natural radioactivity of Australian building materials, industrial wastes and by products.*Health physics*. 48:87–95.
- Biira, S., Kisolo, A.K and D'junga F.M (2014). Concentration levels of radon in mines, industries and dwellings in selected areas of Tororo and Busia districts. *Pelagia research Library; Advances in applied science research*. Vol5(6):31-44

- Busby, C., & Fucic, A.(2006). Ionizing Radiation and Children's Health: Conclusions. *Acta Padiatrica*, 95(453), 81-85.
- Cancer Camp in Tororo. (2013). [www.uci.or.ug/news/82-cancer camp in tororo](http://www.uci.or.ug/news/82-cancer-camp-in-tororo)
- Cathy, V. & Linda, H.,(2008). Human implications of Uranium mining and nuclear power generation.<http://pgs.ca/wp-content/uploads/2008/03/human-health-implications2009-21.pdf>.
- Cember, H., (1996). Introduction to health physics.(3rd edition),McGraw Hill, New York.
- Cember, H. & Johnson, T.E., (2009). Introduction to Health physics. (4th edition), New York: McGraw-Hill Companies, Inc.
- Chege B.W, Gatebe E.G, Mundia C, & Sakurai H. (2014).Activity concentration of ²²⁶Ra, ²³²Th and ⁴⁰K and radiation exposure levels in Nairobi Central business district and the industrial area. *International journal of advanced research*, Vol(2),1035-1040.
- Darwish, I. A., Wani, T. A., Alanazi, A. M., Hamidaddin, M. A., & Zargar, S. (2013). Kinetic-exclusion analysis-based immunosensors versus enzyme-linked immunosorbent assays for measurement of cancer markers in biological specimens. *Talanta*, 111, 13-19.
- Darwish, D. A. E., Abul-Nasr, K. T. M., & El-Khayatt, A. M. (2015). The assessment of natural radioactivity and its associated radiological hazards and dose parameters in granite samples from South Sinai, Egypt. *Journal of Radiation Research and Applied Sciences*, 8(1), 17-25.
- Department of Geological Survey and Mines (2012). Geology and Mineral occurrences in Uganda. Ministry of Energy and Mineral development, Entebbe, *mining journal special publication-Uganda*.
- EPA (2010).Radioactive equilibrium.<http://www.epa.gov>
- Faanu,A, Darko E,O, & Ephrahim, J,H, (2012).Determination of Natural radioactivity and hazard in the soils and rock samples in a mining area in Ghana. *West African journal of ecology*, 19, 77–92
- Faanu, A. Lawluvi, H. Kpeglo D.O, Darko E.O, Emi– Reynolds G, Awudu A.R, Aduku O.K, Kasana C., Ali I.D, Agyman L, & Kpodzro R., (2014). Assessment of natural and anthropogenic radioactivity levels in soils, rocks and water in the vicinity of Chiran Gold mine in Ghana.*Radiation Protection Dosimetry*, 158,87–99
- Fatima, I., Zaidi, J. H., Arif, M., & Tahir, S. N. A. (2006). Measurement of natural radioactivity in bottled drinking water in Pakistan and consequent dose estimates. *Radiation Protection Dosimetry*, 123(2), 234-240.

- Ferdous, J., Rahman, M. M., Rahman, R., Hasan, S., & Ferdous, N. (2015). Radioactivity Distributions in Soils from Habiganj District, Bangladesh and their Radiological Implications. *Malaysian Journal of Soil Science*, 19, 59-71
- Feroz, A.M., & Sajad, A.R.(2015). Measurement of radioactive nuclides present in the soil samples of district Ganderbal of Kashmir province for radiation safety purposes. *Journal of Radiation Research and Applied Sciences* 8 (15):155-159.
- Gbadebo, A.M., (2011). Natural radionuclides distribution in the granitic rocks and soils of abandoned quarry sites, Abeokuta, Southwestern Nigeria. *Asian journal of applied sciences*.4:176–185
- Gilmore, G.R. (2008). *Practical Gamma-Ray Spectroscopy*. 2nd edition, Chichester, England: John Wiley and sons.
- Girigisu S., Ibeanu I.G.E., Adeyemo D.J., Onoja R.A., Bappah I.A., & Okoh S., (2014). Assessment of Radiological levels in soils from Artisan Gold mining exercises at Awwal, Kebbi state, Nigeria. *Research journal of Applied sciences, Engineering and Technology*, 7(14):2899–2904
- Goodman, T.R.,(2010). *Ionizing Radiation Effects and their risks to humans*. Yale University School of medicine. New Haven C.T:www.imagewisely.org. accessed online in November 2014.
- Horst, M., Mariza, R.F., & Lene, H.V., (2013). Acid Rock Drainage and Radiological Environmental impacts, A case study of Uranium mining and milling facilities of Pocos de Caldas. *Journal of waste management*,18: 169-181.
- IAEA (1996) *International Basic Safety Standard for protection against Ionizing radiation and for safety of radiation sources*. Safety series No.115, IAEA, Vienna.
- IAEA (2005). *Naturally occurring radioactive materials (IV)*. Proceedings of the international conference held in Szczyrk. IAEA –TECDOC-1472, Poland
- Ibrahim,N.M. Abdel–Ghani,A.h., Shawky, S.M., Ashiraf, E.M., &Farouk,M.A.,(1993). Measurement of radioactivity levels in soil in the Nile Delta and Middle Egypt. *Health physics journal*. 64,620–627.
- International Commission on Radiological Protection (ICRP). (2000). *Protection of the public in situations of prolonged exposure*; ICRP Publication82; pergamon press, oxford. Ann. ICRP, 29(12)

- Jibiri, N. N., & Okeyode, I. C. (2011). Activity concentrations of natural radionuclides in the sediments of Ogun River, Southwestern Nigeria. *Radiation protection dosimetry*, 147(4), 555-564.
- Kinyua, R., Atambo V.O., & Ongeru, R.M., (2011). Activity concentration of ^{238}U , ^{232}Th and ^{40}K and radiation exposure levels in the Tabaka soapstone quarries of Kisii Region, Kenya African journal of Environmental science and Technology, 5, 682.
- Knoll, G.F.(2000). Radiation detection and measurement, John Wiley & Sons, Inc.USA
- Krane, K.S., (1987). Introductory Nuclear Physics. (2nd edition), John Wiley & Sons, Inc.
- Kuhn. M.A (2003). Oxygen free radicals and anti toxicants. American Journal of natural sciences:103(58-62)
- Laith, A.M., Tawfiq, N.F., & Kitah, F.H., (2013). Measurement of Natural Radioactivity in Building materials used in Iraq. African journal of Basic and Applied sciences.7 (1) :56–66
- Lamarsh, J. R., & Baratta, A. J. (2012). Interaction of Radiation with Matter. *Introduction to Nuclear Engineering*, 52-116.
- L'Annunziata, M.F (2007). Radiactivity. Introduction & History, Amsterdam: Elsevier B.V
- Lilley J. (2002).Nuclear physics principles and applications, second edition, John wiley and sons inc. ISBN 978-0-471-80553-3
- Mattetnik A.B (1995). GDM20-Measurement system for radioactivity. User version 1.2, Gamma Data Mattetnik AB, S-75148, UPPSALA, SWEDEN.
- Moses et.al.,(1990).Radioactive hazards of potable water in Virginia and Maryland. Bull Environ, Contam Toxicol
- Mugaiga,A.,Jurua,E, Oriada,R & Turyahabwa S.E.R(2016).Radiactivity levels and Dose rates from rocks in selected mining areas and quarries in Eastern Uganda. International journal of research in Engineering and technology, 5(3).
- Musoke,R.(2013,February,16). Cancer cases rising in Uganda.
- Mustapha, A.O (1999). Assessment of human exposure to natural sources of radiation in Kenya. PhD thesis (physics). University of Nairobi. Kenya.
- Mazunga, M. S. (2011). Assessment of natural radioactivity and heavy metal levels in the neighborhood of mkuju uranium deposit(Doctoral dissertation, University of Dar es Salaam.).

- Nasiru et al.,(2013). Distribution of Gamma radionuclides in Gold Ore mine from Birnin Gwari Artisanal Goldmine Kaduna state Nigeria. *Research journal of Applied sciences, Engineering and technology* 6(17): 3255-3258.
- Odumo, B.O.,(2009). Radiological survey and Elemental analysis in the Gold mining belt, Southern Nyanza, Kenya. Published masters Dissertation.
- Okeyode, I. C., & Akanni, A. O. (2009). Determination of some physical parameters of Olumo rock, Abeokuta Ogun-State, Nigeria. *Indian Journal of Science and Technology*, 2(7), 6-10.
- Okeyode, I. C., & Oluseye, A. M. (2010). Studies of the Terrestrial Outdoor Gamma Dose Rate Levels in Ogun-Osun River Basins Development Authority Headquarters, Abeokuta, Nigeria. *Physics International*, 1(1), 1-8.
- Osoro et al.,(2011). Radioactivity in surface soils around the proposed sites for Titanium Mining project in Kenya. *Journal of environmental protection*, 2, 460-464
- Xinwei,L. and Zhang, X. (2006). Measurement of natural radioactivity in sand samples collected from Baoji Weihe sand park, china. *Environment Geology* 50:977-982
- Podgorsak, E.B. (2006). *Radiation physics for medical physicists*. Springer-verlag, Berlin, Germany
- Rittersdorf, I. (2007). *Gamma ray spectroscopy*, Moscow, Russia
- Saad M.H, Tamboul, J. and Yousef, M.(2014). Evaluation of natural radioactivity in different regions in Sudan. *Journal of American science*:10(2)
- Saleh,I.H., Hafez, A.F., Elanany, N.H.,Motaweh, H.A & Naim, M.A.,(2007). Radiological study on soils, foodstuff and fertilizers in the Alexandria Region. Egypt. *Turkish journal of Engineering and Environmental science*. 31, 91 –17
- Sterba, J. (2014). *Xenobiology and Toxicology*.University of south Bohemia in the Ceske. Budejovice.
- Taskin, H., Karavus, M. Ay.P., Topuzoglu,A., Hindiroglum,S., & Karahan,G. (2009). Radionuclide concentration in soil and life time cancer risk due to gamma radioactivity in Kirlareli, Turkey. *Journal of Environmental Radioactivity*,100,49-53.
- Tawalbeh,A.A., Samat,S.B., Yasir,M.S., & Omar, M., (2012). Radiological impact of Drinks intake of Naturally Occurring Radionuclides on Adults of Central Zone of Malaysia. Tenth Radiation Physics & Protection Conference, 16(2),187-193.
- Turner, J.E. (2007). *Atoms, Radiation and Radiation Protection*, 3thedition, Wiley-VcH. Weinheim. USA.

- Turyahabwa,S.E.R., Jurua,E., Oriada,R., Mugaiga,A.,& Enjiku,B.D.D(2016). Determination of natural radioactivity levels due to mine tailings from selected mines in southwestern Uganda. *Journal of Environmental and Earth science*: 6(6).
- Uganda Bureau of Statistics (UBOS).(2013) National labour force and child activities survey 2011/2012. *Nationa Labour force survey report,44-48*.
- UNSCEAR (1993).Sources and Effects of Ionizing radiation, United Nations Scientific Committee on the Effects of Atomic Radiation..UNSCEAR, 1993 Report to the General Assembly with scientific annexes. New York, USA: United Nations.
- UNSCEAR. (2000).Sources and Effects of Ionizing radiation, United Nations Scientific Committee on the Effects of Atomic Radiation. Report to the General Assembly with scientific annexes. New York, USA: United Nations
- UNSCEAR. (2011).Sources and Effects of Ionizing radiation, United Nations Scientific Committee on the Effects of Atomic Radiation. Report to the General Assembly with scientific annexes. New York, USA: United Nations
- Veiga,R. Sanches,N. Anjos,R.M., Macario,K., Bastoes,J., Iguatueny, M., et al.2006. Measurement of natural radioactivity in Brazilian Beach sands. *Radiation Measurements*, 41(2), 189–196
- WHO (2013). World Health Organization, ionizing radiation in our environment, online: www.who.int/ionizing radiation/env/en (accessed on 3rd July 2016)
- Yussuf N.M, Hossain I& Wagiran H,(2012). Natural Radioactivity in drinking and mineral water in Johor Bahru (Malaysia).*Scientific research and Essays*; 7(9),1070-1075

APPENDIX A

SPECIFIC ACTIVITIES FOR SOIL AND WATER SAMPLES FROM KASEREM LIMESTONE QUARRY AREA

TABLE A.1: EXTRACTED DATA FROM NaI(TI) DETECTOR FOR SOIL SAMPLES

ID	Mass (g)	t (s)	P K	C	CENT (keV)	SD (keV)	FWHM (keV)	SUM (N)	RAT E	S.A (Bqkg ⁻¹)	ERR OR
	804.8	6019	1	0.0043	118.284	11.371	26.722	1987	0.33	95.39	2.14
	804.8	6019	2	0.0608	198.201	10.808	25.399	7758	1.29	26.34	0.30
CKLA1	804.8	6019	3	0.0237	304.249	24.182	56.827	2594	0.43	22.60	0.44
	804.8	6019	4	0.0101	528.586	36.709	86.267	3669	0.61	74.99	1.24
	804.8	6019	5	0.00234	1268.15	29.064	68.301	7850	1.3	692.54	7.82
	958.85	6545	1	0.0043	105.745	7.291	17.134	956	0.15	35.43	1.15
	958.85	6545	2	0.0608	197.6	12.199	28.667	11886	1.82	31.15	0.29
CKLA2	958.85	6545	3	0.0237	296.894	17.171	40.353	5516	0.84	37.09	0.50
	958.85	6545	4	0.0101	522.914	26.955	63.344	6780	1.04	106.97	1.30
	958.85	6545	5	0.00234	1273.46	45.16	106.125	13455	2.04	916.24	7.90
	944.35	6002	1	0.0043	109.866	8.511	20.001	686	0.11	28.15	1.08
	944.35	6002	2	0.0608	191.844	15.862	37.275	12839	2.14	37.26	0.33
CKLA3	944.35	6002	3	0.0237	300.189	21.844	51.334	2292	0.38	17.06	0.36
	944.35	6002	4	0.0101	523.315	28.472	66.908	5143	0.86	89.84	1.25
	944.35	6002	5	0.00234	1272.44	41.444	97.393	10108	1.68	762.12	7.58
	850	6021	1	0.0043	106.181	8.655	20.338	1108	0.21	50.35	1.51
	850	6021	2	0.0608	198.081	10.777	25.325	8193	1.36	26.33	0.29
CKLA4	850	6021	3	0.0237	295.205	9.516	22.362	1349	0.22	11.12	0.30
	850	6021	4	0.0101	523.907	28.764	67.596	6627	1.1	128.21	1.58
	850	6021	5	0.00234	1275.29	44.832	105.354	10652	1.77	889.46	8.62
	1039.55	6057	1	0.0043	111.276	8.204	19.28	1144	0.19	42.25	1.25
	1039.55	6057	2	0.0608	200.034	19.036	44.734	12412	2.05	32.42	0.29
CKLA5	1039.55	6057	3	0.0237	296.669	17.722	41.646	6929	1.4	46.43	0.56
	1039.55	6057	4	0.0101	522.965	32.513	76.405	7691	1.27	120.94	1.38
	1039.55	6057	5	0.00234	1276.46	51.067	120.008	12528	2.08	850.28	7.60
	977.9	6012	1	0.0043	110.85	10.806	25.395	1342	0.22	53.08	1.44
	977.9	6012	2	0.0608	198.665	11.38	26.744	7969	1.33	22.29	0.25
CKLA6	977.9	6012	3	0.0237	296.703	12.003	28.207	2390	0.44	17.15	0.35
	977.9	6012	4	0.0101	521.491	32.322	75.957	7469	1.24	125.79	1.46
	977.9	6012	5	0.00234	1271.72	35.961	84.509	9088	1.51	660.60	6.93

	1020.35	6001	1	0.0043	108.719	11.749	27.609	1716	0.29	65.17	1.57
CKLA7	1020.35	6001	2	0.0608	198.155	15.442	36.289	9103	1.52	24.45	0.26
	1020.35	6001	3	0.0237	297.633	23.052	54.172	6102	1.02	42.05	0.54
	1020.35	6001	4	0.0101	521.235	30.488	71.646	7293	1.22	117.93	1.38
	1020.35	6001	5	0.00234	1268.73	30.388	71.411	9094	1.52	634.70	6.66
	971.4	6025	1	0.0043	106.023	8.948	21.027	1140	0.19	45.30	1.34
	971.4	6025	2	0.0608	200.258	10.866	25.582	8438	1.4	23.71	0.26
CKLA8	971.4	6025	3	0.0237	302.986	23.575	55.402	2541	0.42	18.32	0.36
	971.4	6025	4	0.0101	528.48	32.559	76.519	8213	1.36	138.94	1.53
	971.4	6025	5	0.00234	1277.45	57.423	134.945	11683	1.94	853.07	7.89
	1007.7	6079	1	0.0043	104.613	8.316	19.544	630	0.1	23.92	0.95
	1007.7	6079	2	0.0608	202.474	16.764	39.397	8212	1.35	22.05	0.24
CKLA9	1007.7	6079	3	0.0237	298.57	22.037	51.786	8638	1.42	59.50	0.64
	1007.7	6079	4	0.0101	519.592	20.323	47.759	3748	0.62	60.58	0.99
	1007.7	6079	5	0.00234	1270.98	35.65	83.778	11205	1.84	781.69	7.39
	1030.5	6001	1	0.0043	104.313	11.113	26.115	1375	0.23	51.71	1.39
	1030.5	6001	2	0.0608	199.678	10.523	24.728	8287	1.38	22.04	0.24
CKLA10	1030.5	6001	3	0.0237	297.75	16.257	38.204	3298	0.55	22.50	0.39
	1030.5	6001	4	0.0101	520.988	23.544	55.328	3750	0.62	60.04	0.98
	1030.5	6001	5	0.00234	1278.62	55.779	131.082	12786	2.13	883.58	7.81
	561.35	6001	1	0.0043	113.068	11.698	27.49	1614	0.27	111.42	2.77
	561.35	6001	2	0.0608	198.161	12.257	28.804	9041	1.51	44.14	0.46
CKLC1	561.35	6001	3	0.0237	292.163	14.13	33.206	2566	0.43	32.14	0.63
	561.35	6001	4	0.0101	520.633	24.835	58.363	2845	0.47	83.62	1.57
	561.35	6001	5	0.00234	1295.64	82.452	193.762	3230	0.54	409.76	7.21
	560.65	6133	1	0.0043	109.429	10.959	25.754	1229	0.2	83.12	2.37
	560.65	6133	2	0.0608	200.382	15.415	36.226	8665	1.41	41.45	0.45
CKLC2	560.65	6133	3	0.0237	289.111	20.864	49.03	5039	0.82	61.83	0.87
	560.65	6133	4	0.0101	520.154	20.466	48.094	2485	0.41	71.56	1.44
	560.65	6133	5	0.00234	1270.73	32.182	75.627	3479	0.57	432.39	7.33
	504.9	6001	1	0.0043	107.188	7.669	18.021	564	0.09	43.29	1.82
	504.9	6001	2	0.0608	202.781	18.818	44.221	7799	1.3	42.34	0.48
CKLC3	504.9	6001	3	0.0237	295.784	18.51	43.498	2203	0.37	30.68	0.65
	504.9	6001	4	0.0101	521.616	23.412	55.017	2813	0.47	91.92	1.73
	504.9	6001	5	0.00234	1277.87	43.535	102.306	1354	0.23	190.97	5.19
	675.05	6512	1	0.0043	109.936	7.772	18.265	726	0.11	38.41	1.43
	675.05	6512	2	0.0608	200.248	15.664	36.81	9433	1.45	35.29	0.36
CKLC4	675.05	6512	3	0.0237	305.69	27.042	63.548	3198	0.49	30.70	0.54

	675.05	6512	4	0.0101	517.586	25.803	60.638	3566	0.55	80.32	1.35
	675.05	6512	5	0.00234	1292.96	78.236	183.855	6235	0.96	606.14	7.68
	533.15	6001	1	0.0043	112.533	7.674	18.034	1235	0.11	89.77	2.55
	533.15	6001	2	0.0608	200.248	15.664	36.81	9433	1.45	48.49	0.50
CKLC5	533.15	6001	3	0.0237	305.69	27.042	63.548	3198	0.49	42.18	0.75
	533.15	6001	4	0.0101	517.586	25.803	60.638	3566	0.55	110.35	1.85
	533.15	6001	5	0.00234	1292.96	78.236	183.855	6235	0.96	832.81	10.55
	554.8	6001	1	0.0043	111.092	7.708	18.113	914	0.15	63.84	2.11
	554.8	6001	2	0.0608	199.693	14.149	33.25	6512	1.09	32.17	0.40
CKLC6	554.8	6001	3	0.0237	297.754	19.598	46.054	3541	0.59	44.88	0.75
	554.8	6001	4	0.0101	544.184	53.083	124.745	2535	0.42	75.39	1.50
	554.8	6001	5	0.00234	1273.51	38.399	90.238	2731	0.46	350.55	6.71
	605.85	6001	1	0.0043	106.605	11.237	26.406	1392	0.23	89.04	2.39
	605.85	6001	2	0.0608	197.027	12.777	30.027	9532	1.59	43.12	0.44
CKLC7	605.85	6001	3	0.0237	297.904	19.674	46.233	1893	0.32	21.97	0.51
	605.85	6001	4	0.0101	549.264	64.635	151.893	5544	0.92	150.98	2.03
	605.85	6001	5	0.00234	1274.96	62.451	146.76	4543	0.76	533.99	7.92
	581.95	6001	1	0.0043	105.542	11.536	27.111	1490	0.25	99.22	2.57
	581.95	6001	2	0.0608	194.292	21.904	51.475	11228	1.87	52.88	0.50
CKLC8	581.95	6001	3	0.0237	299.257	27.634	64.941	4211	0.7	50.88	0.78
	581.95	6001	4	0.0101	546.948	67.604	158.87	4591	0.77	130.16	1.92
	581.95	6001	5	0.00234	1300.57	91.043	213.951	5831	0.97	713.54	9.34
	693.9	6001	1	0.0043	116.147	12.613	29.641	1220	0.22	68.14	1.95
	693.9	6001	2	0.0608	201.521	16.931	39.787	8911	1.48	35.20	0.37
CKLC9	693.9	6001	3	0.0237	300.334	20.29	47.681	5662	0.94	57.37	0.76
	693.9	6001	4	0.0101	555.643	66.678	156.694	4406	0.73	104.76	1.58
	693.9	6001	5	0.00234	1278.65	45.34	106.55	3042	0.51	312.19	5.66
	553.2	6001	1	0.0043	112.162	8.981	21.106	1651	0.28	115.66	2.85
	553.2	6001	2	0.0608	197.851	13.962	32.81	9499	1.58	47.06	0.48
CKLC10	553.2	6001	3	0.0237	300.639	21.308	50.074	2618	0.44	33.28	0.65
	553.2	6001	4	0.0101	558.01	68.433	160.818	3632	0.61	108.32	1.80
	553.2	6001	5	0.00234	1285.03	61.069	143.512	2520	0.42	324.40	6.46
	576.1	6071	1	0.0043	116.811	10.569	24.838	1038	0.18	69.02	2.14
	576.1	6071	2	0.0608	199.877	14.683	34.505	9168	1.51	43.11	0.45
CKLB1	576.1	6071	3	0.0237	298.472	28.769	67.607	5381	0.89	64.92	0.89
	576.1	6071	4	0.0101	567.517	70.68	166.098	5472	0.9	154.91	2.09
	576.1	6071	5	0.00234	1312.89	94.019	220.944	3182	0.52	388.80	6.892
	637	6761	1	0.0043	110.639	9.096	21.376	1456	0.22	78.622	2.060
	637	6761	2	0.0608	197.926	16.577	38.956	12427	1.84	47.458	0.42
CKLB2	637	6761	3	0.0237	292.304	12.78	30.033	3904	0.58	38.25	0.61

	637	6761	4	0.0101	555.554	66.284	155.768	8405	1.24	193.23	2.11
	637	6761	5	0.00234	1332.8	123.82	290.978	6220	0.92	617.20	7.83
	560.65	6068	1	0.0043	106.143	12.855	30.209	1371	0.23	93.72	2.53
	560.65	6068	2	0.0608	200.814	17.482	41.083	9305	1.53	44.99	0.47
CKLB3	560.65	6068	3	0.0237	305.195	27.442	64.488	5426	0.89	67.30	0.91
	560.65	6068	4	0.0101	537.707	55.13	129.555	4895	0.81	142.46	2.04
	560.65	6068	5	0.00234	1306.1	98.533	231.552	5784	0.95	726.57	9.55
	501.2	6091	1	0.0043	109.278	13.077	30.731	1190	0.2	90.65	2.63
	501.2	6091	2	0.0608	198.16	10.928	25.681	9217	1.51	49.66	0.52
CKLB4	501.2	6091	3	0.0237	296.207	16.442	38.638	2258	0.37	31.21	0.66
	501.2	6091	4	0.0101	531.982	46.96	110.356	4608	0.76	149.45	2.20
	501.2	6091	5	0.00234	1304.53	108.308	254.525	4281	0.7	599.28	9.16
	536.1	6010	1	0.0043	114.668	11.284	26.517	1252	0.21	90.37	2.55
	536.1	6010	2	0.0608	196.68	11.002	25.854	9085	1.51	46.38	0.49
CKLB5	536.1	6010	3	0.0237	298.976	22.316	52.442	7033	1.17	92.10	1.10
	536.1	6010	4	0.0101	535.895	54.506	128.089	6795	1.13	208.81	2.53
	536.1	6010	5	0.00234	1322.53	119.646	281.169	6313	1.05	837.34	10.54
	598.9	6010	1	0.0043	112.234	11.376	26.734	1629	0.27	105.25	2.61
	598.9	6010	2	0.0608	197.366	10.556	24.804	8427	1.4	38.51	0.42
CKLB6	598.9	6010	3	0.0237	297.452	17.995	42.289	3738	0.62	43.82	0.72
	598.9	6010	4	0.0101	544.882	64.371	151.272	6226	1.04	171.26	2.17
	598.9	6010	5	0.00234	1324.76	118.946	278.524	6227	1.04	739.32	9.37
	554.65	6011	1	0.0043	107.376	12.475	29.317	1753	0.29	122.28	2.92
	554.65	6011	2	0.0608	196.969	10.513	24.706	9629	1.6	47.50	0.48
CKLB7	554.65	6011	3	0.0237	299.402	27.227	63.985	2819	0.4	35.68	0.67
	554.65	6011	4	0.0101	544.338	66.201	155.571	4522	0.75	134.29	2.00
	554.65	6011	5	0.00234	1328.96	116.215	273.105	5382	0.9	689.86	9.40
	520.75	6898	1	0.0043	111.572	10.237	24.056	1852	0.27	119.90	2.79
	520.75	6898	2	0.0608	198.933	10.848	25.493	10397	1.51	47.61	0.47
CKLB8	520.75	6898	3	0.0237	299.387	24.818	58.322	7229	1.05	84.91	1.00
	520.75	6898	4	0.0101	542.069	59.588	140.033	5481	0.79	151.07	2.04
	520.75	6898	5	0.00234	1338.59	123.612	290.489	6788	0.98	807.56	9.80
	513.7	7163	1	0.0043	112.399	8.813	20.71	1430	0.2	90.38	2.39
	513.7	7163	2	0.0608	197.911	10.297	24.198	8988	1.25	40.18	0.42
CKLB9	513.7	7163	3	0.0237	299.381	23.353	54.878	2585	0.36	29.64	0.58
	513.7	7163	4	0.0101	541.203	62.84	147.674	4002	0.56	107.68	1.70
	513.7	7163	5	0.00234	1290.96	78.935	185.498	5286	0.74	613.91	8.44
	578.6	6984	1	0.0043	111.497	9.779	22.98	1577	0.23	90.76	2.29
	578.6	6984	2	0.0608	198.304	10.112	23.762	10271	1.47	41.81	0.41

CKLB10	578.6	6984	3	0.0237	299.422	20.29	47.681	2872	0.41	29.99	0.56
	578.6	6984	4	0.0101	547.426	66.179	155.521	5621	0.8	137.72	1.84
	578.6	6984	5	0.00234	1318.19	105.974	249.04	6708	0.96	709.41	8.66
	499.1	6728	1	0.0043	109.777	12.262	28.817	1365	0.2	94.54	2.56
	499.1	6728	2	0.0608	199.747	12.633	29.688	8705	1.29	42.64	0.46
CKLD1	499.1	6728	3	0.0237	302.24	20.379	47.892	5442	0.81	68.38	0.93
	499.1	6728	4	0.0101	555.773	66.442	156.139	4351	0.65	128.29	1.95
	499.1	6728	5	0.00234	1315.09	95.636	224.744	4886	0.73	621.82	8.90
	558.35	6008	1	0.0043	108.037	7.454	17.508	937	0.16	64.96	2.12
	558.35	6008	2	0.0608	197.632	9.246	21.727	5933	0.99	29.09	0.38
CKLD2	558.35	6008	3	0.0237	301.082	18.223	42.825	2760	0.46	34.72	0.66
	558.35	6008	4	0.0101	551.463	69.846	164.13	3147	0.52	92.88	1.66
	558.35	6008	5	0.00234	1275.07	19.192	45.102	1503	0.25	191.47	4.94
	547.9	6299	1	0.0043	111.81	10.348	24.318	1080	0.17	72.78	2.21
	547.9	6299	2	0.0608	199.023	12.735	29.927	9046	1.44	43.11	0.45
CKLD3	547.9	6299	3	0.0237	298.435	21.323	50.108	6208	0.99	75.90	0.96
	547.9	6299	4	0.0101	532.706	42.394	99.625	4421	0.7	126.83	1.91
	547.9	6299	5	0.00234	1273.31	18.251	42.89	1188	0.19	147.11	4.27
	591.4	6104	1	0.0043	111.73	6.383	15.001	285	0.05	18.36	1.09
	591.4	6104	2	0.0608	203.062	15.93	37.435	8417	1.38	38.35	0.42
CKLD4	591.4	6104	3	0.0237	294.011	15.344	36.058	4816	0.79	56.29	0.81
	591.4	6104	4	0.0101	549.834	60.057	141.134	7785	1.28	213.52	2.42
	591.4	6104	5	0.00234	1273.86	24.163	56.782	1614	0.26	191.07	4.76
	615.3	6037	1	0.0043	107.572	10.524	24.732	1991	0.33	124.65	2.79
	615.3	6037	2	0.0608	199.015	9.735	22.878	12287	2.04	54.40	0.49
CKLD5	615.3	6037	3	0.0237	300.188	18.111	42.561	4636	0.77	52.66	0.77
	615.3	6037	4	0.0101	542.829	55.461	130.334	5913	0.98	157.61	2.05
	615.3	6037	5	0.00234	1327.09	106.566	250.431	4083	0.68	469.74	7.35
	617.15	6045	1	0.0043	104.568	12.11	28.459	1500	0.25	93.51	2.41
	617.15	6045	2	0.0608	201.833	16.053	37.724	8841	1.46	38.98	0.42
CKLD6	617.15	6045	3	0.0237	297.688	18.38	43.194	4909	0.81	55.52	0.79
	617.15	6045	4	0.0101	542.549	61.541	144.621	4516	0.75	119.85	1.78
	617.15	6045	5	0.00234	1274.32	17.019	39.995	1286	0.21	147.31	4.11
	694	6024	1	0.0043	111.145	12.362	29.051	1824	0.3	101.46	2.38
	694	6024	2	0.0608	198.278	10.547	24.786	12324	2.05	48.49	0.44
CKLD7	694	6024	3	0.0237	296.501	10.451	24.559	3642	0.6	36.76	0.61
	694	6024	4	0.0101	516.686	21.585	50.724	5105	0.85	120.90	1.69
	694	6024	5	0.00234	1273.57	15.523	36.479	317	0.05	32.40	1.82
	673.15	6015	1	0.0043	111.802	8.511	20.000	924	0.15	53.07	1.75

	673.15	6015	2	0.0608	198.817	11.197	26.314	10895	1.81	44.26	0.42
CKLD8	673.15	6015	3	0.0237	303.458	20.24	47.563	3229	0.54	33.65	0.59
	673.15	6015	4	0.0101	530.387	37.468	88.05	3969	0.66	97.05	1.54
	673.15	6015	5	0.00234	1278.11	38.366	90.16	1213	0.2	128.03	3.68
	572.2	6001	1	0.0043	114.61	9.005	21.161	1148	0.19	77.75	2.30
	572.2	6001	2	0.0608	199.842	11.72	27.541	7989	1.33	38.27	0.43
CKLD9	572.2	6001	3	0.0237	299.414	14.271	33.537	2131	0.36	26.19	0.57
	572.2	6001	4	0.0101	517.791	31.069	73.011	3190	0.53	91.98	1.63
	572.2	6001	5	0.00234	1282.7	46.246	108.679	2656	0.44	330.55	6.41
CKLD10	602.15	6002	1	0.0043	109.751	13.119	30.829	1401	0.23	90.15	2.41
	602.15	6002	2	0.0608	197.993	12.36	29.046	10391	1.73	47.29	0.46
	602.15	6002	3	0.0237	298.384	19.841	46.626	3013	0.5	35.18	0.64
	602.15	6002	4	0.0101	560.074	68.335	160.588	5368	0.89	147.06	2.01
	602.15	6002	5	0.00234	1328.34	112.552	264.497	5157	0.86	609.79	8.49
CKLE1	531.2	6005	1	0.0043	166.55	30.193	70.93	790	0.13	57.60	2.05
	531.2	6005	2	0.0608	254.84	13.629	31.028	2407	0.40	12.41	0.25
	531.2	6005	3	0.0237	299.54	14.843	53.83	2451	0.41	32.42	0.66
	531.2	6005	4	0.0101	532.248	28.957	65.695	2626	0.44	81.51	1.59
	531.2	6005	5	0.00234	1231.68	116.283	103.934	3337	0.56	447.06	7.74
CKLE2	560.32	6002	1	0.0043	104.181	8.655	20.338	980	0.16	67.77	2.17
	560.32	6002	2	0.0608	197.081	10.777	25.325	3362	0.56	16.44	0.28
	560.32	6002	3	0.0237	295.205	9.516	22.362	2330	0.39	29.23	0.61
	560.32	6002	4	0.0101	523.907	28.764	67.596	3034	0.51	89.32	1.62
	560.32	6002	5	0.00234	1275.29	44.832	105.354	3267	0.54	415.15	7.26
CKLE3	600.25	6020	1	0.0043	108.866	9.511	21.001	876	0.15	56.38	1.91
	600.25	6020	2	0.0608	192.844	17.862	38.275	3212	0.53	14.62	0.26
	600.25	6020	3	0.0237	300.189	21.844	51.334	2598	0.43	30.34	0.60
	600.25	6020	4	0.0101	523.315	28.472	67.908	3415	0.57	93.57	1.60
	600.25	6020	5	0.00234	1282.44	42.444	98.393	2710	0.45	320.50	6.16
CKLE4	500.25	6000	1	0.0043	106.188	8.669	19.021	1140	0.19	88.33	2.62
	500.25	6000	2	0.0608	201.781	19.818	45.221	2715	0.45	14.88	0.29
	500.25	6000	3	0.0237	295.784	19.51	43.498	2890	0.48	40.63	0.76
	500.25	6000	4	0.0101	531.616	23.412	55.017	2976	0.50	98.17	1.80
	500.25	6000	5	0.00234	1276.87	43.535	101.306	3938	0.66	560.69	8.94
CKLE5	498.24	6008	1	0.0043	103.313	12.113	27.115	987	0.16	76.68	2.44
	498.24	6008	2	0.0608	200.678	11.523	25.728	2568	0.43	14.11	0.28
	498.24	6008	3	0.0237	298.75	16.257	38.204	2715	0.45	38.27	0.73
	498.24	6008	4	0.0101	521.988	22.544	53.328	3579	0.60	118.38	1.98
	498.24	6008	5	0.00234	1272.62	55.779	131.082	2976	0.50	424.86	7.79

CKLE6	505.38	6001	1	0.0043	113.234	10.376	27.734	1210	0.20	92.78	2.67
	505.38	6001	2	0.0608	198.366	11.556	24.804	2690	0.45	14.59	0.28
	505.38	6001	3	0.0237	296.452	12.995	42.289	2650	0.44	36.87	0.72
	505.38	6001	4	0.0101	545.882	63.371	151.272	3467	0.58	113.19	1.92
	505.38	6001	5	0.00234	1323.76	118.946	273.524	2900	0.48	408.64	7.59
CKLE7	540.12	6010	1	0.0043	108.429	10.959	22.754	1140	0.19	81.67	2.42
	540.12	6010	2	0.0608	201.382	14.415	37.226	3100	0.52	15.71	0.28
	540.12	6010	3	0.0237	288.111	20.864	50.03	2810	0.47	36.53	0.69
	540.12	6010	4	0.0101	521.154	21.466	49.094	3445	0.57	105.08	1.79
	540.12	6010	5	0.00234	1272.73	31.182	76.627	3750	0.62	493.69	8.06
CKLE8	499.45	6004	1	0.0043	106.188	7.669	19.021	980	0.16	76.00	2.43
	499.45	6004	2	0.0608	201.781	17.818	43.221	2986	0.50	16.38	0.30
	499.45	6004	3	0.0237	294.784	19.51	42.498	2987	0.50	42.03	0.77
	499.45	6004	4	0.0101	522.616	22.412	56.017	3549	0.59	117.18	1.97
	499.45	6004	5	0.00234	1288.87	44.535	104.306	3690	0.61	525.87	8.66
CKLE9	516.35	6020	1	0.0043	107.936	8.772	19.265	1040	0.17	77.81	2.41
	516.35	6020	2	0.0608	205.248	14.664	37.81	2459	0.41	13.01	0.26
	516.35	6020	3	0.0237	308.69	28.042	66.548	2645	0.44	35.90	0.70
	516.35	6020	4	0.0101	519.586	24.803	61.638	3456	0.57	110.08	1.87
	516.35	6020	5	0.00234	1296.96	77.236	184.855	3540	0.59	486.68	8.18
CKLE10	507.65	6002	1	0.0043	116.533	7.674	19.034	990	0.16	75.56	2.40
	507.65	6002	2	0.0608	203.248	14.664	37.81	2890	0.48	15.60	0.29
	507.65	6002	3	0.0237	303.69	26.042	62.548	2770	0.46	38.36	0.73
	507.65	6002	4	0.0101	518.586	24.803	60.638	3520	0.59	114.38	1.93
	507.65	6002	5	0.00234	1282.96	76.236	182.855	3810	0.63	534.38	8.66

TABLE A.2: EXTRACTED DATA FROM NaI(Tl) DETECTOR FOR WATER SAMPLES

ID	Mass(g)	t(s)	C	Cent (KeV)	S.D	FWHM	SUM(N)	Rate	S.A	ERROR
CKLS1	504.2	6007	0.0043	127.565	15.58	36.614	1159	0.19	88.99	2.61
	504.2	6007	0.0608	196.214	15.206	35.735	822	0.12	4.46	0.16
	504.2	6007	0.0237	308.668	21.231	49.892	1318	0.22	18.36	0.51
	504.2	6007	0.0101	535.105	15.857	37.263	442	0.07	14.45	0.69
	504.2	6007	0.00234	1400.788	46.576	109.447	32	0.01	4.52	0.80
CKLS2	524.2	6058	0.0043	126.766	7.421	17.439	341	0.06	24.97	1.35
	524.2	6058	0.0608	199.757	15.239	35.812	857	0.14	4.44	0.15
	524.2	6058	0.0237	303.193	10.671	25.076	1101	0.18	14.63	0.44
	524.2	6058	0.0101	533.842	9.676	22.738	140	0.02	4.36	0.37
	524.2	6058	0.00234	1435.76	25.942	60.963	26	0	3.50	0.69
CKLS3	526.69	6001	0.0043	134.152	22.219	52.215	1653	0.28	121.63	2.99
	526.69	6001	0.0608	194.392	14.859	34.92	1191	0.2	6.20	0.18
	526.69	6001	0.0237	301.288	13.299	31.254	947	0.16	12.64	0.41
	526.69	6001	0.0101	530.73	12.76	29.985	158	0.03	4.95	0.39
	526.69	6001	0.00234	1404.167	37.895	82.003	16	0	2.16	0.54
CKLS4	521.55	6135	0.0043	135.175	24.239	56.962	1765	0.29	128.28	3.05
	521.55	6135	0.0608	206.255	10.822	25.431	564	0.09	2.90	0.12
	521.55	6135	0.0237	308.198	16.135	37.917	1065	0.17	14.04	0.43
	521.55	6135	0.0101	556.651	36.011	84.625	503	0.08	15.56	0.69
	521.55	6135	0.00234	1376.969	70.432	165.515	148	0.02	19.77	1.62
CKLS5	524.7	6230	0.0043	130.617	17.946	42.174	1397	0.22	99.39	2.66
	524.7	6230	0.0608	192.218	11.557	27.158	472	0.08	2.37	0.11
	524.7	6230	0.0237	317.126	31.179	73.272	939	0.15	12.12	0.40
	524.7	6230	0.0101	530.301	25.497	59.918	944	0.15	28.59	0.93
	524.7	6230	0.00234	1399.525	45.294	106.441	247	0.04	32.29	2.05
CKLP1	524.7	6050	0.0043	113.168	7.987	18.762	905	0.15	66.30	2.20
	524.7	6050	0.0608	192.706	12.241	28.767	1279	0.21	6.63	0.19
	524.7	6050	0.0237	305.732	15.043	35.352	2126	0.35	28.26	0.61
	524.7	6050	0.0101	533.723	20.308	47.725	1342	0.22	41.86	1.14
	524.7	6050	0.00234	1419.619	34.253	80.493	126	0.02	16.96	1.51
CKLP2	524.8	6566	0.0043	135.212	23.156	54.419	2618	0.4	176.69	3.45
	524.8	6566	0.0608	204.657	9.301	21.858	805	0.12	3.84	0.14
	524.8	6566	0.0237	304.645	11.505	27.037	1722	0.26	21.09	0.51
	524.8	6566	0.0101	535.719	16.782	39.436	1352	0.21	38.85	1.06
	524.8	6566	0.00234	1419.021	51.942	122.065	484	0.07	60.03	2.73
CKLP3	529.2	6331	0.0043	134.746	17.954	42.192	965	0.15	66.98	2.16
	529.2	6331	0.0608	197.469	13.049	30.665	808	0.13	3.97	0.14
	529.2	6331	0.0237	310.959	17.966	42.219	2210	0.35	27.83	0.59
	529.2	6331	0.0101	540.268	33.834	79.511	2244	0.35	66.31	1.40
	529.2	6331	0.00234	1435.77	42.795	100.568	414	0.07	52.81	2.60

CKLP4	528.1	6074	0.0043	124.118	15.34	36.049	1980	0.33	143.55	3.23
	528.1	6074	0.0608	201.222	8.454	19.866	735	0.12	3.77	0.14
	528.1	6074	0.0237	306.937	15.266	35.876	1844	0.3	24.26	0.56
	528.1	6074	0.0101	534.897	23.489	55.199	1452	0.24	44.82	1.18
	528.1	6074	0.00234	1430.723	52.725	123.904	175	0.03	23.31	1.76
CKLP5	526.95	6002	0.0043	128.724	16.657	39.144	1700	0.28	125.00	3.03
	526.95	6002	0.0608	195.98	17.707	41.619	1188	0.2	6.18	0.18
	526.95	6002	0.0237	303.463	11.061	25.993	1454	0.24	19.40	0.51
	526.95	6002	0.0101	535.998	16.674	39.177	865	0.14	27.08	0.92
	526.95	6002	0.00234	1448.075	21.358	50.192	88	0.01	11.89	1.27

APPENDIX B

SPECIFIC ACTIVITIES AND GRAPHS

4.1.B :SPECIFIC ACTIVITIES FOR SOIL SAMPLES FROM THE CENTRE OF THE QUARRY (A)

TABLE 4.1.B: Specific activities of soil samples from the central part of the quarry denoted as (A)

ID	SPECIFIC ACTIVITY (Bqkg^{-1})							
	Ra-226		Th-232		U-238		K-40	
CKLA1	95.39	± 2.14	49.27	± 0.75	22.59	± 0.44	692.53	± 7.82
CKLA2	35.43	± 1.15	67.41	± 0.78	37.09	± 0.50	916.24	± 7.90
CKLA3	28.15	± 1.07	61.58	± 0.77	17.06	± 0.36	762.11	± 7.58
CKLA4	50.35	± 1.51	75.87	± 0.92	11.12	± 0.30	889.46	± 8.62
CKLA5	42.25	± 1.25	74.96	± 0.82	46.43	± 0.56	850.28	± 7.60
CKLA6	53.08	± 1.45	72.86	± 0.84	17.15	± 0.35	660.60	± 6.93
CKLA7	65.17	± 1.57	69.89	± 0.81	42.05	± 0.54	634.70	± 6.66
CKLA8	45.30	± 1.34	80.07	± 0.88	18.32	± 0.36	853.07	± 7.89
CKLA9	23.92	± 0.95	40.15	± 0.60	59.50	± 0.64	781.69	± 7.38
CKLA10	51.71	± 1.39	39.87	± 0.60	22.50	± 0.39	883.58	± 7.81
MEAN	49.08	± 1.38	63.19	± 0.78	29.38	± 0.44	792.43	± 7.62
STDEV	20.40	± 0.33	16.85	± 0.11	15.87	± 0.11	101.84	± 0.55
STERR	6.45	± 0.10	5.33	± 0.04	5.02	± 0.03	32.21	± 0.17

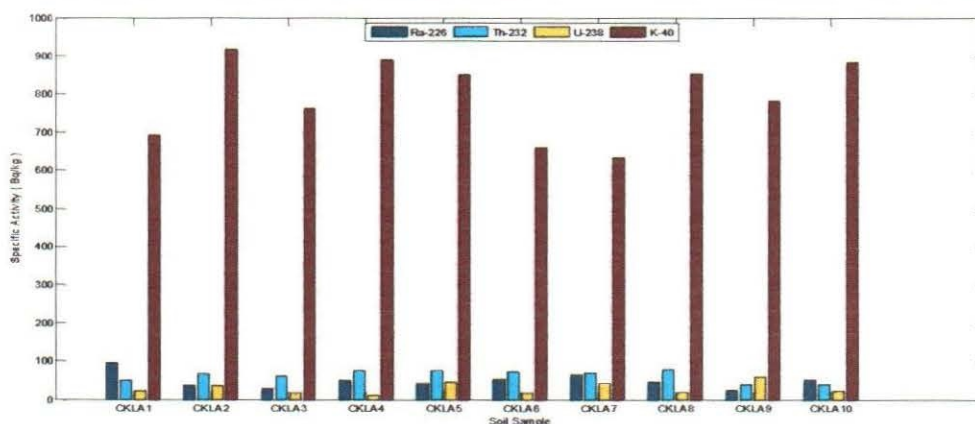


FIGURE 4.1.B Specific activities of soil from the Central part of the quarry

4.2.B: SPECIFIC ACTIVITY OF SOIL FROM A RADIUS OF 50 m AWAY FROM THE CENTRE OF THE QUARRY (A)

TABLE 4.2.B: Specific activities of soil from a radius of 50 m away from the centre of the quarry called (B)

ID	SPECIFIC ACTIVITY (Bqkg ⁻¹)			
	Ra-226	Th-232	U-238	K-40
CKLB1	69.02 ± 2.14	96.73 ± 1.25	64.92 ± 0.88	388.80 ± 6.89
CKLB2	78.62 ± 2.06	117.83 ± 1.24	38.25 ± 0.61	617.20 ± 7.83
CKLB3	93.72 ± 2.53	91.34 ± 1.23	67.30 ± 0.91	726.57 ± 9.55
CKLB4	90.65 ± 2.63	96.92 ± 1.33	31.21 ± 0.66	599.28 ± 9.16
CKLB5	90.37 ± 2.55	125.14 ± 1.48	92.10 ± 1.10	837.34 ± 10.54
CKLB6	105.25 ± 2.61	102.85 ± 1.27	43.82 ± 0.72	739.32 ± 9.37
CKLB7	122.28 ± 2.92	88.38 ± 1.21	35.68 ± 0.67	689.86 ± 9.40
CKLB8	119.90 ± 2.79	96.82 ± 1.23	84.91 ± 1.00	807.56 ± 9.80
CKLB9	90.38 ± 2.39	71.80 ± 1.04	29.64 ± 0.58	613.91 ± 8.44
CKLB10	90.76 ± 2.29	87.55 ± 1.10	29.99 ± 0.56	709.41 ± 8.66
MEAN	95.09 ± 2.49	97.54 ± 1.24	51.78 ± 0.77	672.92 ± 8.96
STDEV	16.65 ± 0.27	16.35 ± 0.13	23.64 ± 0.19	127.71 ± 1.05
STERR	5.26 ± 0.09	5.17 ± 0.04	7.48 ± 0.06	40.39 ± 0.33

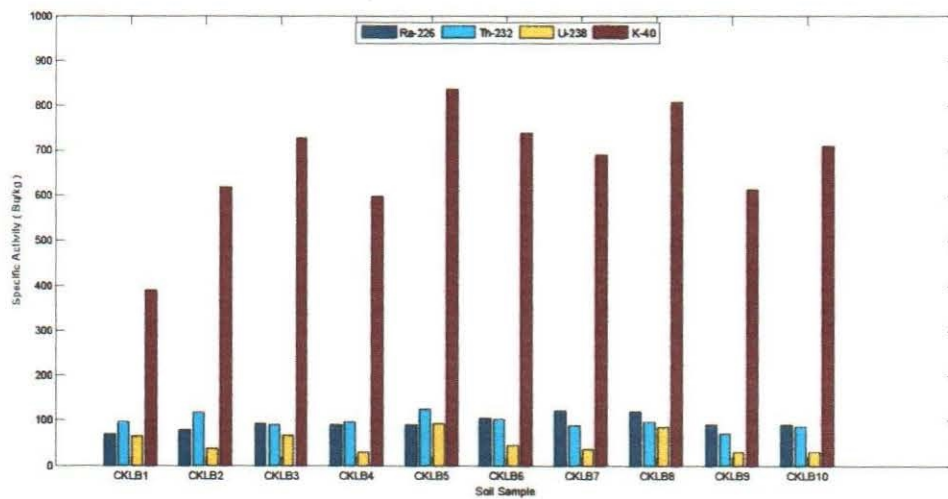


FIGURE 4.2.B: Specific activities of soil samples from a radius of 50 m away from the centre of the quarry (A)

4.3.B: SPECIFIC ACTIVITIES OF SOIL FROM A RADIUS OF 100 m AWAY FROM THE CENTRE OF THE QUARRY (A)

TABLE 4.3.B: Specific activities of soil from a radius of 100 m away from the centre of the quarry called (C)

ID	SPECIFIC ACTIVITY (Bqkg ⁻¹)			
	Ra-226	Th-232	U-238	K-40
CKLC1	111.42 ± 2.77	61.54 ± 0.99	32.14 ± 0.63	409.76 ± 7.21
CKLC2	83.12 ± 2.37	54.31 ± 0.92	61.83 ± 0.87	432.39 ± 7.33
CKLC3	43.29 ± 1.82	64.89 ± 1.08	30.68 ± 0.65	190.97 ± 5.19
CKLC4	38.41 ± 1.43	55.94 ± 0.83	30.70 ± 0.54	606.14 ± 7.68
CKLC5	89.77 ± 2.55	76.86 ± 1.15	42.18 ± 0.75	832.81 ± 10.55
CKLC6	63.84 ± 2.11	52.08 ± 0.93	44.88 ± 0.75	350.55 ± 6.71
CKLC7	89.04 ± 2.39	94.77 ± 1.21	21.97 ± 0.50	534.00 ± 7.92
CKLC8	99.22 ± 2.57	88.72 ± 1.18	50.88 ± 0.78	713.54 ± 9.34
CKLC9	68.14 ± 1.95	68.12 ± 0.96	57.37 ± 0.76	312.19 ± 5.66
CKLC10	115.66 ± 2.85	75.20 ± 1.11	33.27 ± 0.65	324.40 ± 6.46
MEAN	80.19 ± 2.28	69.24 ± 1.04	40.59 ± 0.69	470.67 ± 7.41
STDEV	26.45 ± 0.45	15.64 ± 0.13	13.03 ± 0.11	199.12 ± 1.61
STERR	8.36 ± 0.14	4.95 ± 0.04	4.12 ± 0.04	62.97 ± 0.51

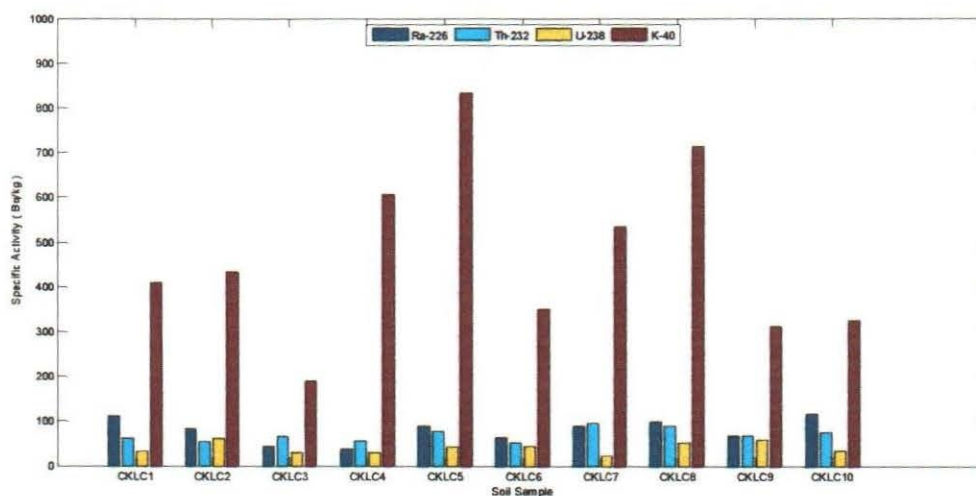


FIGURE 4.3.B: Specific activities of soil samples from a radius of 100 m from the centre of the quarry (A)

4.4.B: SPECIFIC ACTIVITY OF SOIL SAMPLES FROM A RADIUS OF 150m AWAY FROM THE CENTRE OF THE QUARRY (A)

TABLE 4.4 B: Specific activities of soil samples from a radius of 150 m from the central part of the quarry denoted as (D)

ID	SPECIFIC ACTIVITY (Bqkg ⁻¹)							
	Ra-226		Th-232		U-238		K-40	
CKLD1	94.53	± 2.56	83.21	± 1.18	68.38	± 0.93	621.82	± 8.90
CKLD2	64.96	± 2.12	59.45	± 1.00	34.72	± 0.66	191.47	± 4.94
CKLD3	72.78	± 2.21	82.69	± 1.16	75.90	± 0.96	147.11	± 4.27
CKLD4	18.36	± 1.09	123.91	± 1.40	56.29	± 0.81	191.07	± 4.76
CKLD5	124.65	± 2.79	103.13	± 1.24	52.66	± 0.77	469.74	± 7.35
CKLD6	93.51	± 2.41	77.35	± 1.08	55.52	± 0.79	147.31	± 4.11
CKLD7	101.46	± 2.38	82.13	± 1.04	36.76	± 0.61	32.40	± 1.82
CKLD8	53.07	± 1.75	68.31	± 0.96	33.65	± 0.59	128.03	± 3.68
CKLD9	77.75	± 2.29	63.10	± 1.01	26.19	± 0.57	330.55	± 6.41
CKLD10	90.15	± 2.41	94.67	± 1.21	35.18	± 0.64	609.79	± 8.49
MEAN	79.12	± 2.20	83.79	± 1.13	47.52	± 0.73	286.93	± 5.47
STDEV	29.35	± 0.48	21.45	± 0.14	16.63	± 0.14	210.58	± 2.26
STERR	9.28	± 0.15	6.78	± 0.05	5.26	± 0.04	66.59	± 0.71

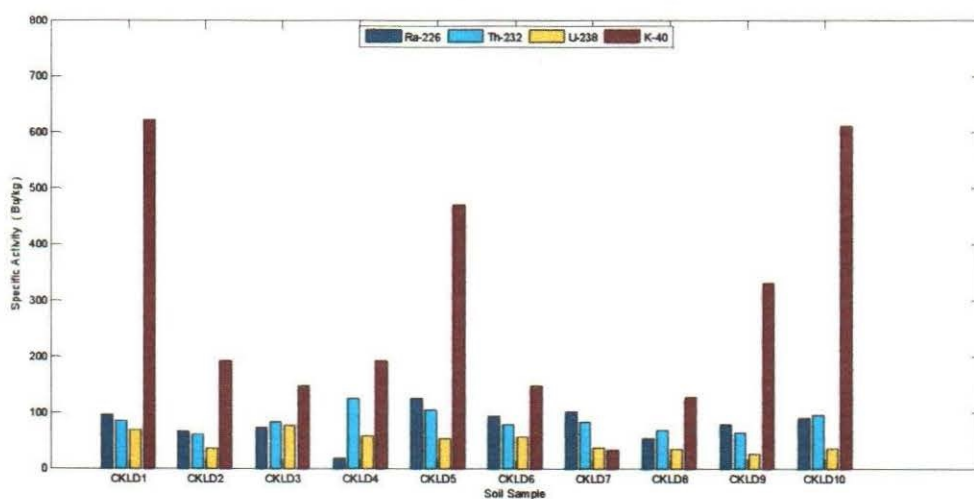


FIGURE 4.4.B: Specific activities of soil samples from a radius of 150 m away from the centre of the quarry (A)

4.5.B: SPECIFIC ACTIVITY OF SOIL SAMPLES FROM A RADIUS OF 600m AWAY FROM THE CENTRE OF THE QUARRY (A)

TABLE 4.5.B: Specific activities of soil samples from a radius of 600 m away from the central part of the quarry called (E)

ID	SPECIFIC ACTIVITY (Bqkg ⁻¹)			
	Ra-226	Th-232	U-238	K-40
CKLE1	57.60 ± 2.05	46.30 ± 0.91	32.42 ± 0.65	447.06 ± 7.74
CKLE2	67.77 ± 2.16	52.01 ± 0.94	29.23 ± 0.61	415.15 ± 7.26
CKLE3	56.38 ± 1.90	53.32 ± 0.92	30.34 ± 0.60	320.50 ± 6.16
CKLE4	88.33 ± 2.62	55.74 ± 1.03	40.63 ± 0.76	560.69 ± 8.93
CKLE5	76.68 ± 2.44	65.50 ± 1.11	38.27 ± 0.73	424.86 ± 7.79
CKLE6	92.78 ± 2.67	63.11 ± 1.09	36.87 ± 0.72	408.64 ± 7.59
CKLE7	81.67 ± 2.42	59.56 ± 1.02	36.53 ± 0.69	493.69 ± 8.06
CKLE8	76.00 ± 2.43	65.91 ± 1.12	42.03 ± 0.77	525.87 ± 8.66
CKLE9	77.81 ± 2.41	60.86 ± 1.05	35.90 ± 0.70	486.68 ± 8.18
CKLE10	75.56 ± 2.40	64.17 ± 1.09	38.36 ± 0.73	534.38 ± 8.66
MEAN	75.06 ± 2.35	58.65 ± 1.03	36.06 ± 0.69	461.75 ± 7.90
STDEV	11.80 ± 0.24	7.00 ± 0.08	4.22 ± 0.06	72.52 ± 0.81
STERR	3.73 ± 0.08	2.21 ± 0.03	1.33 ± 0.02	22.93 ± 0.26

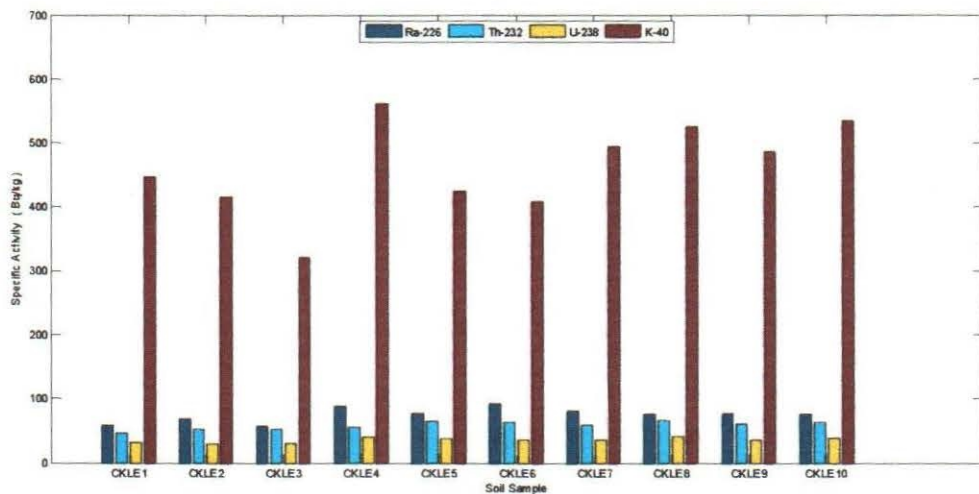


FIGURE 4.5.B: Specific activities of soil samples from a radius of 600 m away from the centre of the quarry (A)

TABLE 4.6.B: Overall Mean Specific Activities of Radionuclides for each location stated above around the quarry

ID	SPECIFIC ACTIVITY (Bqkg ⁻¹)			
	Ra-226	Th-232	U-238	K-40
CKLA(centre)	49.08 ± 1.38	64.69 ± 0.79	29.38 ± 0.44	792.43 ± 7.62
CKLB(50m)	95.09 ± 2.49	99.90 ± 1.26	51.78 ± 0.77	672.92 ± 8.96
CKLC(100m)	80.19 ± 2.28	71.48 ± 1.06	40.59 ± 0.69	470.67 ± 7.41
CKLD(150m)	79.12 ± 2.20	89.73 ± 1.41	47.52 ± 0.73	286.93 ± 5.47
CKLE(600m)	75.06 ± 2.35	59.23 ± 1.04	36.06 ± 0.69	461.75 ± 7.90
TOTAL MEAN	75.71 ± 2.14	77.01 ± 1.11	41.07 ± 0.67	536.94 ± 7.47
STDEV	20.93 ± 0.35	15.46 ± 0.12	14.68 ± 0.12	142.36 ± 1.25

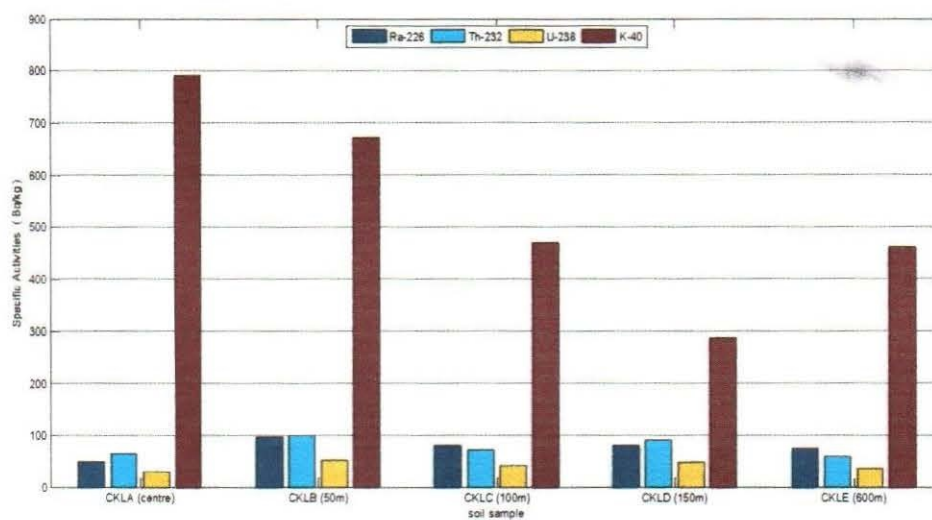


FIGURE 4.6.B: Mean activities for the sampled locations around the quarry

TABLE 4.7.B: TABLE OF SPECIFIC ACTIVITIES FOR RUNNING SURFACE WATER

ID	SPECIFIC ACTIVITY (Bqkg ⁻¹)			
	Ra-226	Th-232	U-238	K-40
CKLS1	88.99 ± 2.61	9.46 ± 0.42	18.36 ± 0.51	4.52 ± 4.52
CKLS2	24.97 ± 1.35	4.40 ± 0.26	14.63 ± 0.44	3.50 ± 3.50
CKLS3	121.63 ± 2.99	5.57 ± 0.29	12.64 ± 0.41	2.16 ± 2.16
CKLS4	128.28 ± 3.05	9.23 ± 0.41	14.04 ± 0.43	19.77 ± 19.77
CKLS5	99.39 ± 2.66	15.48 ± 0.52	12.12 ± 0.40	32.29 ± 32.29
MEAN	92.65 ± 2.53	8.83 ± 0.38	14.36 ± 0.44	12.45 ± 12.45
STDEV	41.07 ± 0.69	4.33 ± 0.11	2.46 ± 0.04	13.19 ± 13.19
STEER	18.37 ± 0.31	1.94 ± 0.05	1.10 ± 0.02	5.90 ± 5.90

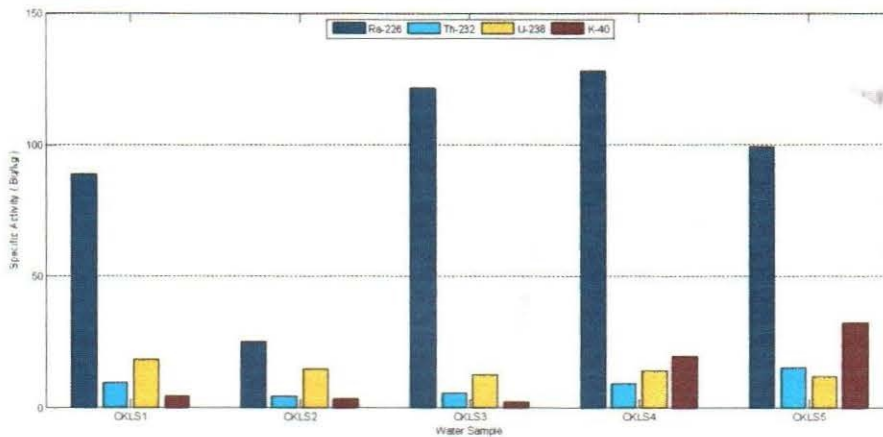


FIGURE 4.7.B: Specific activities of water samples picked from the stream (Running surface water source)

TABLE 4.8.B: TABLE OF SPECIFIC ACTIVITIES FOR PROTECTED SPRING

ID	SPECIFIC ACTIVITY (Bqkg ⁻¹)			
	Ra-226	Th-232	U-238	K-40
CKLP1	66.30 ± 2.20	24.24 ± 0.66	28.26 ± 0.61	16.96 ± 1.51
CKLP2	176.69 ± 3.45	21.34 ± 0.60	21.09 ± 0.51	60.03 ± 2.73
CKLP3	66.98 ± 2.16	35.14 ± 0.77	27.83 ± 0.59	52.81 ± 2.60
CKLP4	143.55 ± 3.23	24.29 ± 0.66	24.26 ± 0.56	23.31 ± 1.76
CKLP5	125.00 ± 3.03	16.63 ± 0.55	19.40 ± 0.51	11.89 ± 1.27
MEAN	115.70 ± 2.81	24.33 ± 0.65	24.17 ± 0.56	33.00 ± 1.97
STDEV	48.46 ± 0.60	6.80 ± 0.08	3.95 ± 0.05	21.90 ± 0.65
STEER	21.67 ± 0.27	3.04 ± 0.04	1.77 ± 0.02	9.80 ± 0.29

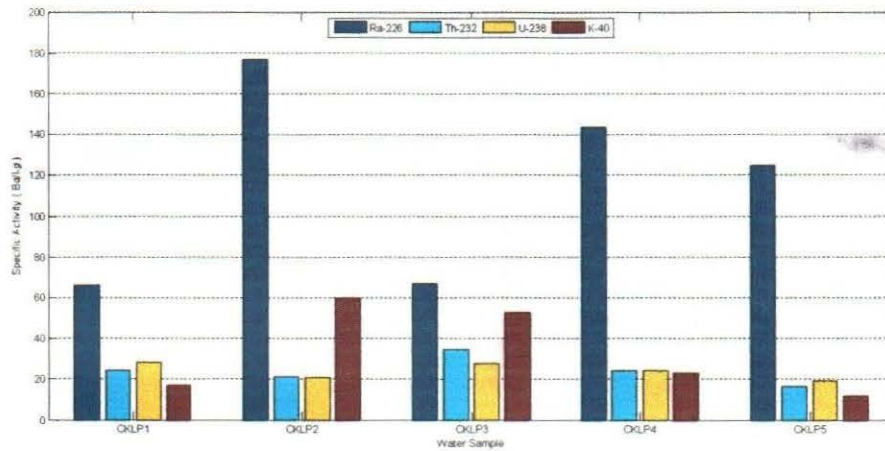


FIGURE 4.8.B: Specific activities of water samples picked from the spring (Protected under ground water)

TABLE 4.9.B : Overall Mean activities for water samples

ID	SPECIFIC ACTIVITY (Bqkg ⁻¹)			
	Ra-226	Th-232	U-238	K-40
CKLS	92.65 ± 2.53	8.83 ± 0.38	14.36 ± 0.44	12.45 ± 1.14
CKLP	115.70 ± 2.81	24.33 ± 0.65	24.17 ± 0.56	33.00 ± 1.97
MEAN	104.18 ± 2.67	16.58 ± 0.52	19.27 ± 0.50	22.73 ± 1.56
STDEV	44.77 ± 0.64	5.57 ± 0.09	3.20 ± 0.05	17.55 ± 0.66

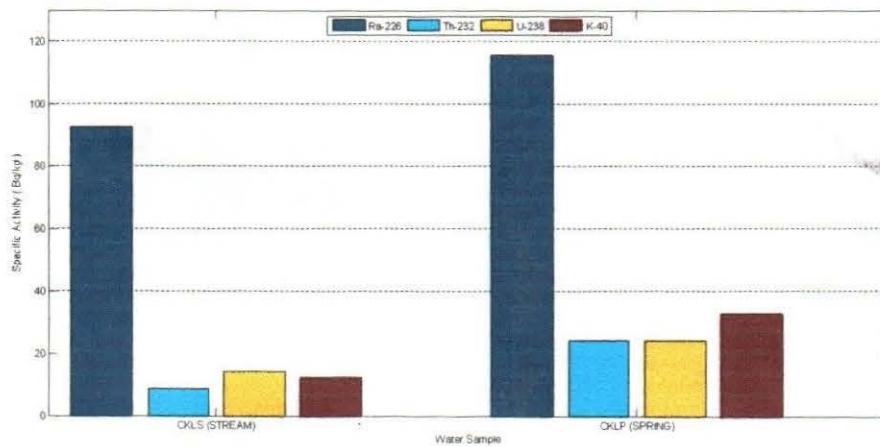


FIGURE 4.9.B: Mean specific activities of water samples collected from both the stream and protected spring

TABLE 4.10.B: showing Radiological Indices

SAMPLE ID	Ra_{eq} (Bqkg ⁻¹)			D(nGhr ⁻¹)			AED(mSvy ⁻¹)			H_{ex} (Bqkg ⁻¹)			H_{in} (Bqkg ⁻¹)		
SOIL															
CKLA	202.60	±	3.10	97.85	±	1.44	0.27	±	0.00	0.55	±	0.01	0.68	±	0.01
CKLB	289.77	±	4.99	135.68	±	2.29	0.39	±	0.01	0.78	±	0.01	1.04	±	0.02
CKLC	218.64	±	4.37	101.80	±	1.99	0.29	±	0.01	0.59	±	0.01	0.81	±	0.02
CKLD	229.53	±	4.63	105.53	±	2.11	0.31	±	0.01	0.62	±	0.01	0.83	±	0.02
CKLE	195.31	±	4.44	91.11	±	2.03	0.26	±	0.01	0.53	±	0.01	0.73	±	0.02
WATER															
CKLS	106.24	±	3.16	45.94	±	1.38	0.14	±	0.00	0.29	±	0.01	0.54	±	0.02
CKLP	153.04	±	3.89	66.93	±	1.72	0.21	±	0.01	0.41	±	0.01	0.73	±	0.02

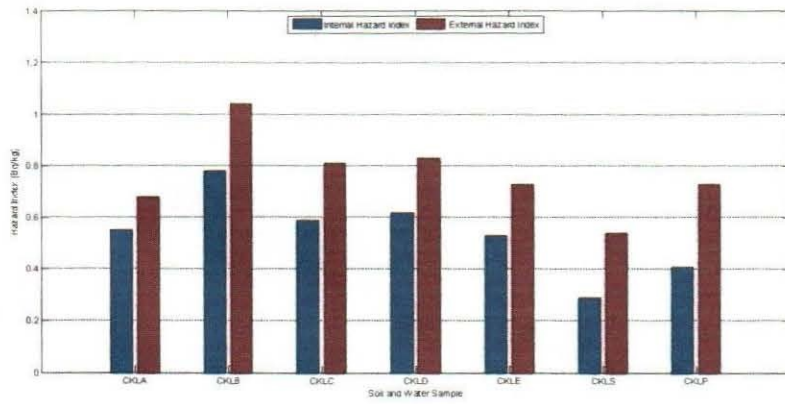


FIGURE 4.10.B: Hazard Indices

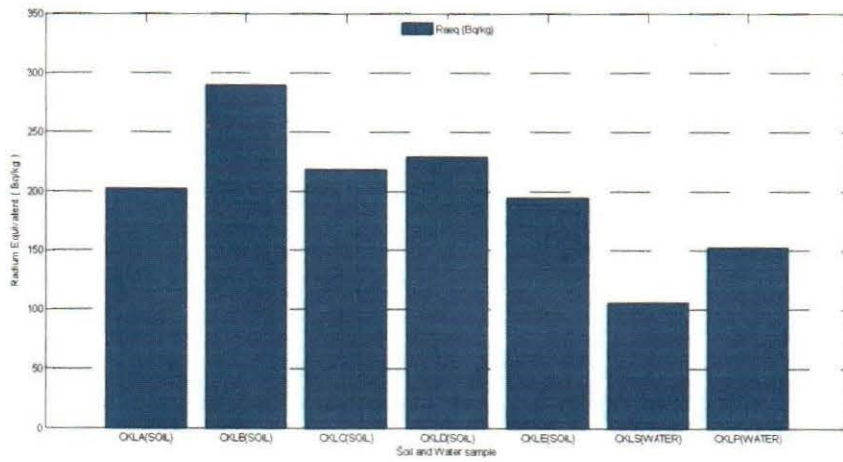


FIGURE 4.10.B: Radium Equivalents